



FINAL PUBLISHABLE REPORT

Grant Agreement number 15SIB10
 Project short name MetroBeta
 Project full title Radionuclide beta spectra metrology

Project start date and duration:		01 June 2016, 36 months
Coordinator: Dr Mark A. Kellett, CEA		Tel: +33 1 6908 2776
Project website address: http://metrobeta-empir.eu		E-mail: mark.kellett@cea.fr
Internal Funded Partners:	External Funded Partners:	Unfunded Partners:
1. CEA, France	4. Gonitec, Netherlands	7. CHUV, Switzerland
2. CMI, Czech Republic	5. UHEI, Germany	
3. PTB, Germany	6. UMCS, Poland	
RMG: -		



TABLE OF CONTENTS

1	Overview	3
2	Need	3
3	Objectives	3
4	Results	4
5	Impact	32
6	List of publications.....	33

1 Overview

The project MetroBeta aimed to improve knowledge of beta spectra, through both theoretical and experimental approaches. Existing theoretical knowledge was used to account for the nuclear structure effects on beta spectra and a new code BetaShape was produced. Experiments were performed using four types of devices: i) specifically developed cryogenic metallic magnetic calorimeters (MMCs), operating at very low temperature, ii) solid scintillators, iii) a magnetic spectrometer and iv) silicon lithium (SiLi) detectors. Comparison of the calculated and measured spectra was performed to validate the quality of the spectra and the improved theory. The effect of this improved knowledge on the measurement of the activity (the becquerel) of beta emitting radionuclides was demonstrated.

2 Need

In the development of new nuclear reactors and in light of the increasing quantity of nuclear waste from existing reactors, the requirements on the diagnostics of nuclear reactor cores and nuclear waste management are becoming more and more stringent. In particular, the calculation of decay heat upon reactor shutdown and in nuclear waste requires improved knowledge of the energy of the beta emissions. The intended monitoring of the isotopic composition of reactor cores via measurement of the anti-neutrino spectrum are dependent on the precise determination of individual beta spectra.

In nuclear medicine, the number of radionuclides being utilised in the fight against cancer is increasing. The available information for these radionuclides can be uncertain, particularly for new applications. In the case of beta emitters, a precise knowledge of the energy spectra is of paramount importance since the physiological impact varies strongly with energy. Thus, poorly known beta spectra can lead to large discrepancies in the effective dose.

There is also an increasing demand for precision beta spectrometry from several fields of fundamental research, such as in the direct measurement of the neutrino mass and in nuclear astrophysics.

Finally, the metrology of ionising radiation was another main driver for this project, since the SI derived unit for activity, the becquerel, is determined via very precise primary activity measurements which crucially depend on the knowledge of the shape of the beta spectra.

3 Objectives

This project aimed to meet the above needs and to improve knowledge of the energy of the particles emitted during the beta decay process, by providing a validated computer code to enable precise predictions for all types of beta spectra, including reliable uncertainties.

This project addressed the following scientific and technical objectives:

1. To improve modern measurement techniques for silicon detectors (Si(Li)), solid scintillator crystals (LaBr₃/CeBr₃) and magnetic spectrometers for measurements of beta spectra.
2. To optimise beta spectrometers, based on metallic magnetic calorimeters (MMCs), and measure high resolution beta spectra for low (< 100 keV) and intermediate (< 1 MeV) end-point energy pure beta emitters Sm-151, C-14, Tc-99 and Cl-36.
3. To improve theoretical computation methods on the basis of the measured spectra and compare the measured and calculated beta spectra.
4. To investigate the effect of improved beta spectra on absolute activity measurements and measure Bremsstrahlung cross-sections to quantify their effect.
5. To facilitate the take up of the technology and measurement infrastructure developed by the project by the measurement supply chain (accredited laboratories, instrumentation manufacturers) and end users (the nuclear medicine community and the nuclear power industry).

4 Results

Availability of beta spectra

The BetaShape code, which has been further developed by CEA within this project, has been used to provide beta spectra for two major international nuclear decay data evaluation projects. The International Atomic Energy Agency's (IAEA) *International Network of Nuclear Structure and Decay Data Evaluators* (NSDD), provides both plots and tabulated beta spectra calculated with the BetaShape code. These spectra are available from the *Live Chart of Nuclides* tool available at: <https://www-nds.iaea.org/relnsd/vcharthtml/VChartHTML.html>. A second international collaboration, the Decay Data Evaluation Project (DDEP), who provide decay scheme data mainly to the metrology community, have also made available the tabulated data for the beta spectra calculated with the BetaShape code at: <http://www.inhb.fr/nuclear-data/nuclear-data-table/>.

Improvement of modern measurement techniques for silicon detectors (Si(Li)), solid scintillator crystals (LaBr₃/CeBr₃) and magnetic spectrometers for measurements of beta spectra.

Improvements in the use of three current measurement techniques have been implemented and more precise beta spectra have been measured.

Beta spectra measured with a Si(Li) detector

The precise characterisation of the physical dimensions of the Si(Li) detector was achieved by X-raying the detector and housing, and a detailed and accurate Monte Carlo model was created by CMI. The model was then used to characterise the detector response prior to the measurement of the beta spectra for seven radionuclides: P-32, Cl-36, Sr-89, Sr-90, Y-90, Pm-147 and Tl-204 and the beta spectra of a variety of Y-90/Sr-90 mixtures. A specially designed and purpose-built collimator was used in order to reduce the distortion to the measured spectra.

The beta spectra were measured by CMI for the radionuclides P-32, Cl-36, Sr-89, Sr-90, Y-90, Pm-147, and additionally Tl-204. The measured spectra were compared with spectra calculated by Monte Carlo method using MCNP code. Because of insufficient agreement between measured and calculated spectrum for Cl-36, additional spectrum of Tl-204 was measured.

Spectra measured by CMI for individual radionuclides are in the Figures 1 to 7. Good agreement between measured and calculated spectra is for all radionuclides except Cl-36. The difference for Cl-36 was very probably caused by the sample shape with too much active mass, because of long half-life of the radionuclide and amount of activity needed for measurement.

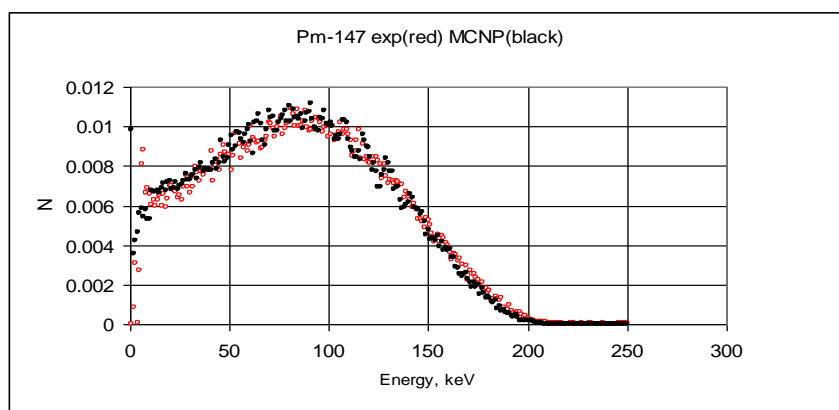


Figure 1: Measured (exp) and calculated (MCNP) beta spectra of Pm-147

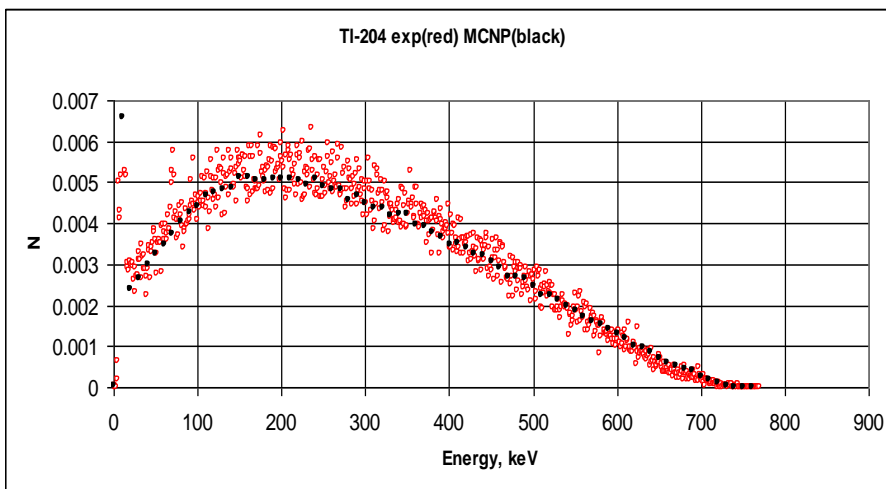


Figure 2: Measured (exp) and calculated (MCNP) beta spectra of TI-204

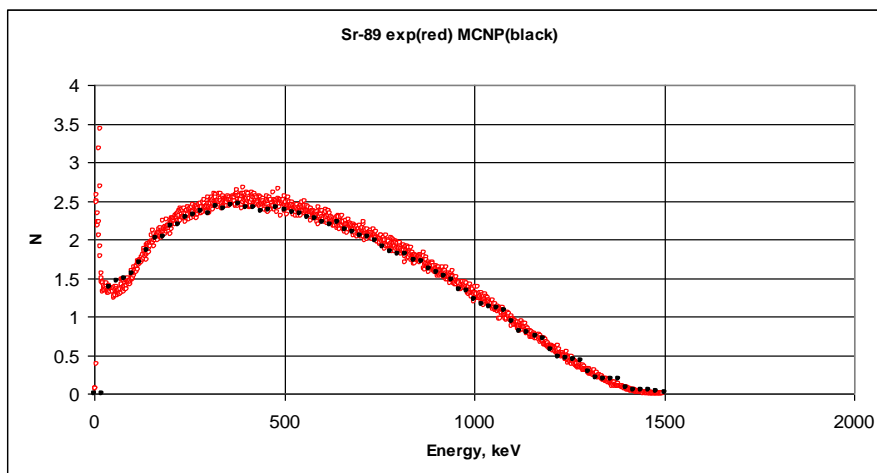


Figure 3: Measured (exp) and calculated (MCNP) beta spectra of Sr-89

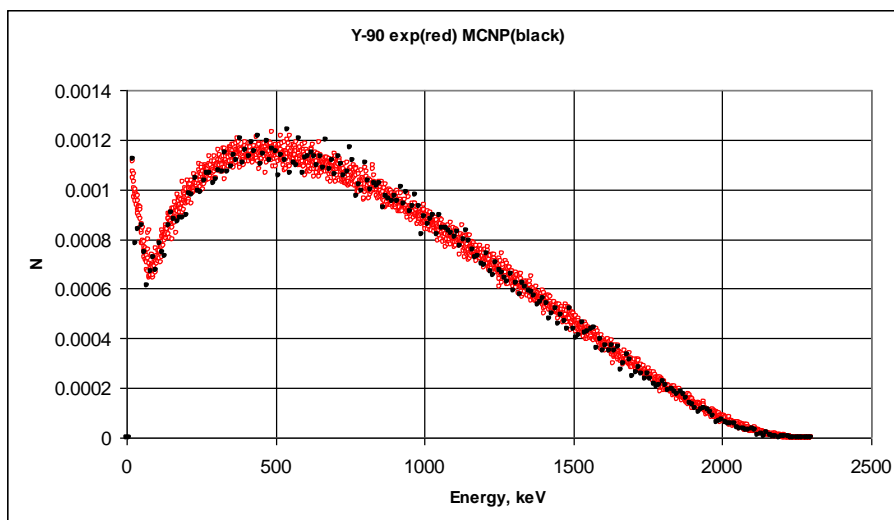


Figure 4: Measured (exp) and calculated (MCNP) beta spectra of Y-90

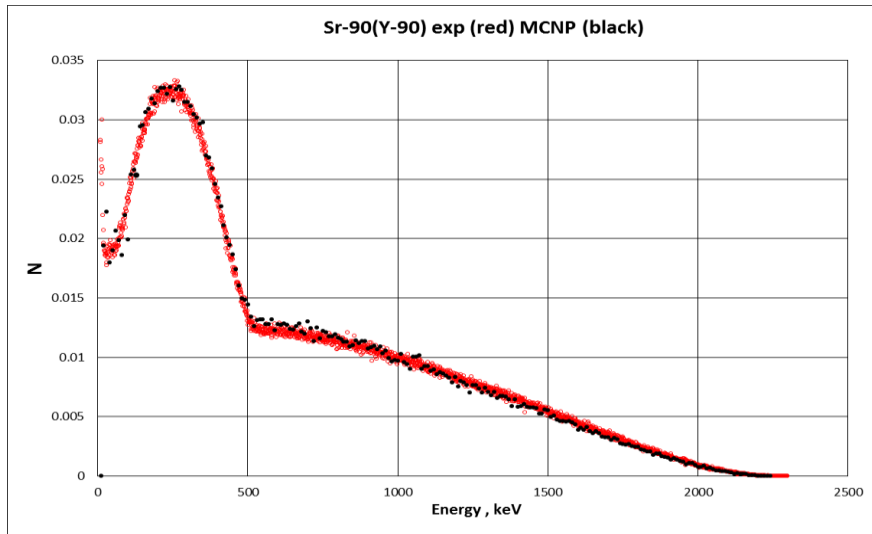


Figure 5: Measured (exp) and calculated (MCNP) beta spectra of Sr-90 (Y-90)

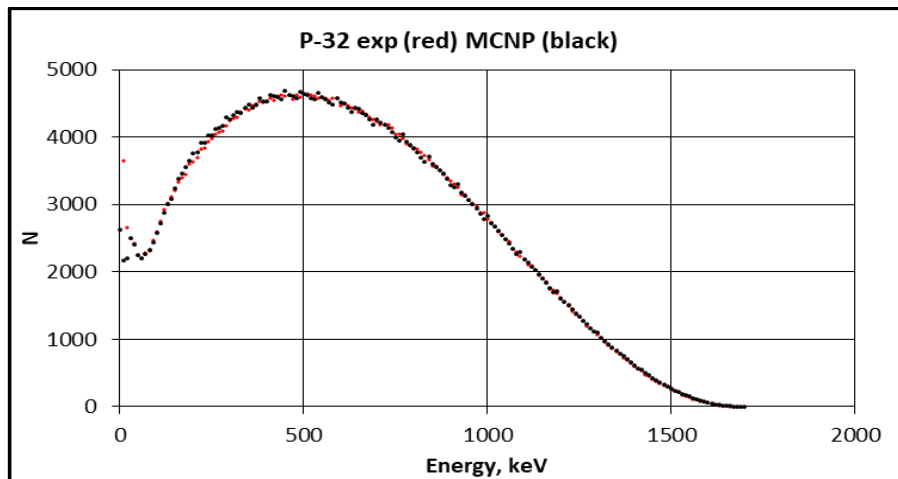


Figure 6: Measured (exp) and calculated (MCNP) beta spectra of P-32

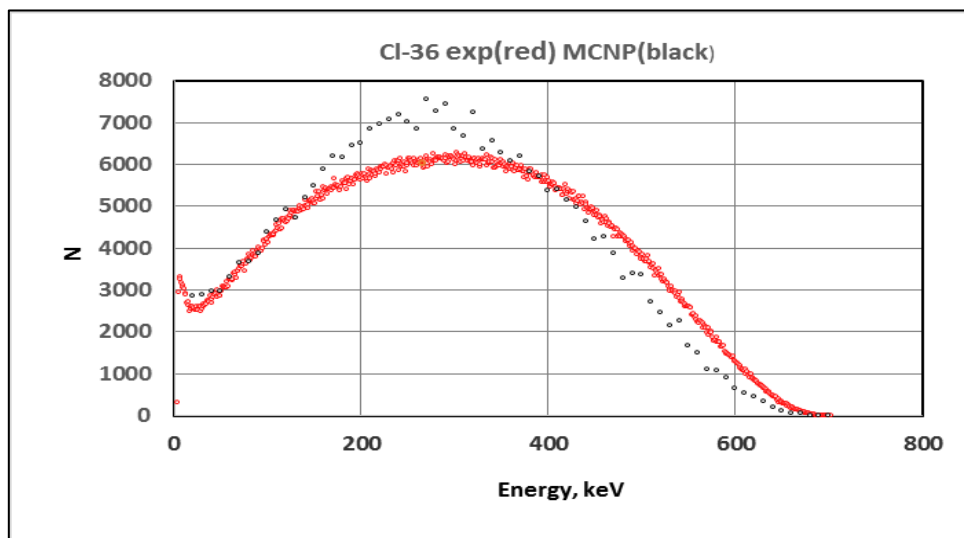


Figure 7: Measured (exp) and calculated (MCNP) beta spectra of Cl-36

Beta spectra measured with solid scintillator crystals

The solid scintillator crystal development work by Gonitec has led to the successful measurement of the Lu-176 and Rb-87 beta spectra through developments in the data acquisition system, for which a dedicated lead-castle-based acquisition set up was implemented and characterised.

Originally, the task was intended to focus exclusively on measurements of Lu-176 however, measurements of Rb-87 also took place. Both nuclides are long-lived primordial nuclides and undergo beta decay transitions of the non-unique kind with half-lives of over 10^{10} years.

Lu, and hence Lu-176, is present in a wide range of solid scintillator crystals (SSCs) therefore preliminary measurements and investigations were devoted to select the most performing SSC compounds and to establish the most effective measurement technique for Lu-176 beta spectroscopy. Tested SSCs include LSO (Lu_2SiO_5), LuAG ($\text{LuAl}_5\text{O}_{12}$), LuAP (LuAlO_3) and LuYAG ($(\text{Lu}_{0.75}\text{Y}_{0.25})_3\text{Al}_5\text{O}_{12}$). LSO and LuAG were then chosen for advanced measurements of Lu-176 also in reason of the complementarity of their scintillator characteristics.

Lu-176 presents a rather complex beta decay which includes a cascade Hf-176 de-excitation emissions of gamma rays and conversion electrons (CE). The most probable beta transition of Lu-176 has a relative probability of 99.6 % and an end point energy of about 600 keV. This beta transition has been the main focus of the task however measurement of the less probable transition (0.4 % relative probability) was also performed and analysed.

In order to establish the most effective measurement technique for Lu-176 a number of criteria were considered by Gonitec, such as the capability to obtain sufficient counting statistics in practical acquisition times (typically no more than a few weeks) and the ability to trigger efficient gamma/beta coincidence. The above led to the need of using relatively small samples of the order of 1 cm^3 and to the need of detecting the beta in coincidence with the emission of the lowest de-excitation of Hf-176 corresponding to 88 keV. The latter condition, in turn, required the development of dedicated post-processing analytical techniques able to unfold the 88 keV signature from the acquired beta spectrum shape. Available literature on spectrum unfolding and de-convolution techniques was used to develop the needed analytical tools however numerous adaptations to specific Lu-176/SSC characteristics had to be implemented from scratch. The final results turned out at the end very satisfactory, however in the meantime, in order to mitigate the risks of uncertain outputs, measurements of Rb-87 were undertaken as well.

Rb-87 measurements were performed by Gonitec using two prototype samples of RbGd_2Br_7 . Since Rb-87 is a pure beta emitter no conditional coincidences are possible and the measurements have to deal with unavoidable presence of background affecting the lower energy part of the spectrum below 10 keV. Efforts led again to satisfactory results both in terms of measurements of beta spectrum shape as well as in the point of view of advancing the SSC technique.

The main task achievements in terms of measured beta spectra are listed below and detailed one by one in the following pages. Details on the measurements and associated experimental and analytical techniques along with advances in the SSC technique applied to beta decay spectroscopy are reported in the relevant Good Practice Guide.

- Experimental shape factors of Lu-176 main beta transition
- Experimental end point evaluation of Lu-176 main beta transition
- Measurement and evaluation of the less probable beta transition of Lu-176
- Experimental shape factor of Rb-87 from 12 keV to end point with high accuracy
- Experimental shape factor of Rb-87 from 2 keV to end point
- End point evaluation of Rb-87

Figure 8 shows the spectrum of the main beta transition of Lu-176 collected by Gonitec with the LuAG sample with dimension of $8 \times 8 \times 8 \text{ mm}^3$ and using an advanced experimental setup consisting of a specifically designed pen-type PMT allowing fitting inside a well-type NaI(Tl) scintillator detector for enhanced coincidence counting efficiency (nearly full solid angle). Both the measured spectrum and the resulting spectrum after application of dedicated analytical unfolding techniques are shown.

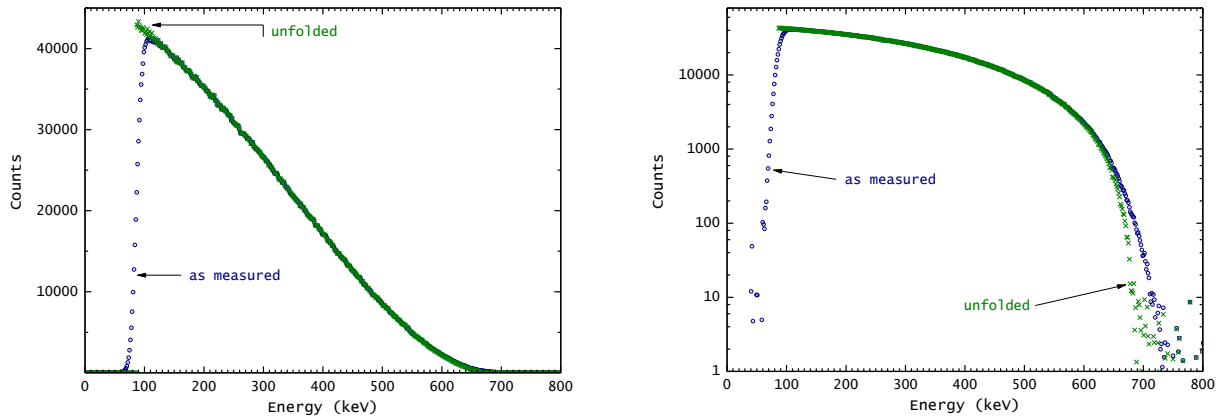


Figure 8: Measured and unfolded beta spectrum of Lu-176 main beta transition collected with a 8x8x8 mm³ LuAG

The spectrum is recorded as a convolution of the beta plus 88 keV corresponding to gamma/electron conversion. Based on the data of Figure 9 experimental shape factors of Lu-176 are parametrised as: $1 - 0.463 W - 0.751 W^{-1} + 0.085 W^2 + 0.276 W^{-2}$.

Confirmed by measurement with both LSO and LuAG and with samples of different sizes, the endpoint of Lu-176 is found at an energy slightly larger than that obtained by atomic mass evaluation, i.e. 601.6 keV vs 597.3 keV. The end point is determined with the Kurie plot shown in Figure 9 referring to the same 8x8x8 mm³ LuAG sample as above. The bottom part of the figure shows in terms of linear fit residuals how the end point value by atomic mass evaluation, albeit just few keV smaller, is incompatible with the present experimental data.

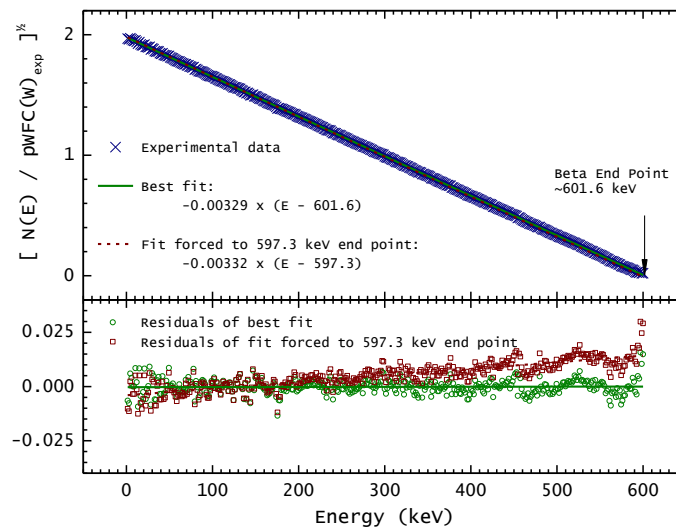


Figure 9: Kurie plot and end point determination of Lu-176 main beta transition with data from the 8x8x8 mm³ LuAG sample.

Figure 10 shows the spectrum of the Lu-176 minor beta transition collected with the same crystal as used for the main transition and the corresponding Kurie plot in Figure 11. The end point evaluation is in line with that of the main beta transition and is again a few keV larger than the value reported by atomic mass evaluation, 200 keV vs 196.3 keV respectively.

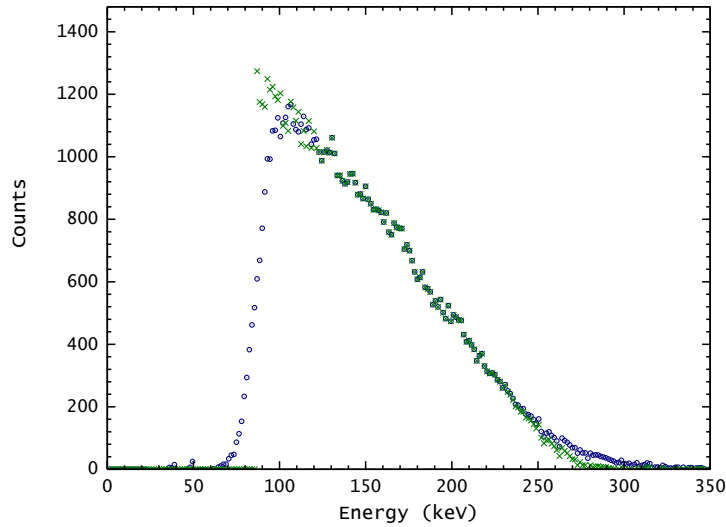


Figure 10: Measurement of the Lu-176 minor beta transition with a 8x8x8 mm³ LuAG sample. Acquisition time is over 30 days for less than 100,000 counts. Blue dots are the spectrum as measured and green crosses the unfolded spectrum.

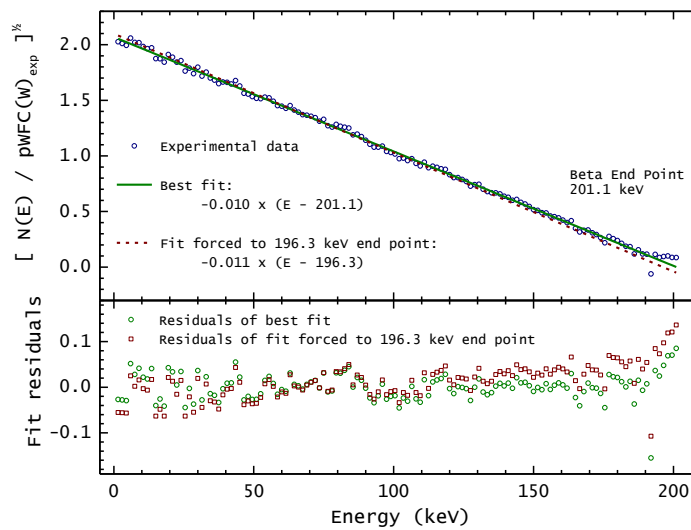


Figure 11: Kurie plot and end point determination of the Lu-176 minor beta transition with data from the 8x8x8 mm³ LuAG sample and lower part the residuals of the fit forced to the atomic mass evaluated end point (196.3 keV) are reported showing as starting at about 100 keV this fit tends to deviate from the experimental data.

Measurements of Rb-87 were performed by Gonitec with two SSC samples of RbGd₂Br₇, however, due to the relatively low Rb-87 count rate achieved by the crystals (several Bq) the lower energy part of the spectrum (as shown in Figure 12) is affected by presence of electronic noise and by environmental radiation recorded using a small CsI(Tl) SSC sample. High accuracy of the measurements can be achieved only for energies above 12 keV where, as seen in Figure 12, there is no significant background able to distort the beta shape.

Derived experimental shape factors are plotted in Figure 13 along with best fit based on the existing parametrisation obtained in the energy range 65 keV to 180 keV, which is in good agreement with the present work in that energy range. Beta spectrum shape from Grau Carles, 2007, and the present work are also compared in Figure 14.

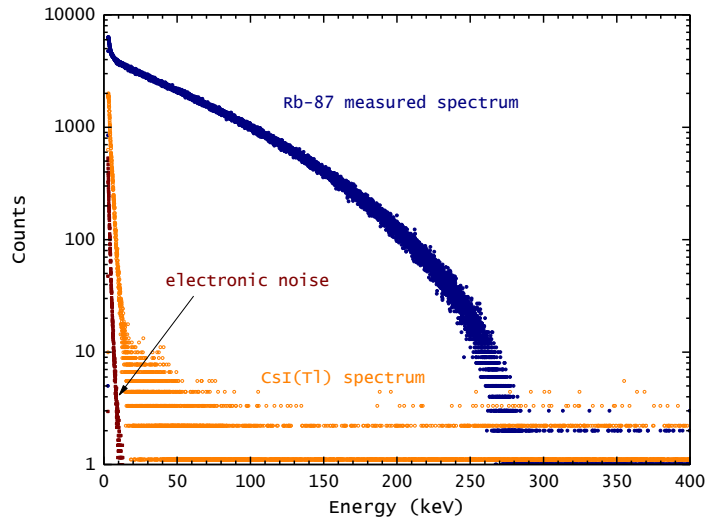


Figure 12: Measured beta spectrum with RbGd₂Br₇ blue dots. Contribution of electronic noise is also shown along with that of environmental radiation as measured with a CsI(Tl) SSC.

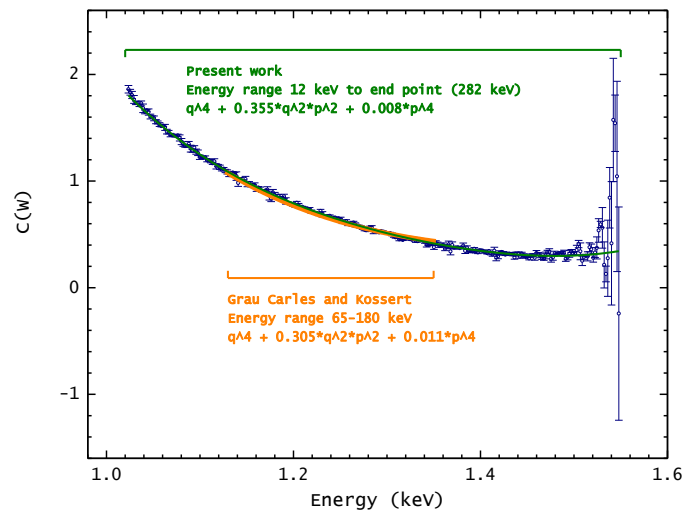


Figure 13: Experimental shape factors for Rb-87 (data point) and their best fit covering the energy range 12 keV to endpoint (green line). The shape factor parametrisation from Grau Carles, 2007, is also reported in its actually detected energy range from 65 keV to 180 keV (orange line).

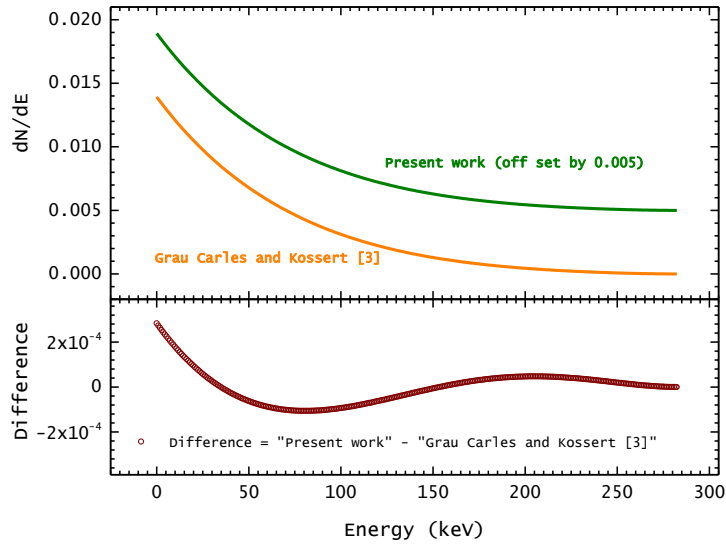


Figure 14: Comparison of the present work shape factors and that from Grau Carles, 2007, on the computational beta spectrum in the all energy range of Rb-87. The present work curve is offset by 0.05 for better visualisation.

More measurements were performed by Gonitec with emphasis on the ability to precisely characterise and then subtract the noise and background affecting the lower energy region of the spectrum. A model to correct for the scintillation non-proportionality of the response was included in the analytical tool for spectrum unfolding. A shape factor parametrisation covering the energy spectrum from 2 keV to the end point is then found as:

$$q^4 + 0.348 q^2 p^2 + 0.008 p^4$$

It can be seen in Figure 15 that the very low energy part is not precisely fitted which can be due to a combination of ineffective noise and background subtraction and/or unprecise scintillation non-proportionality of the response correction and/or non-inclusion in the available computational spectrum of fine corrections as that for electron exchange effects.

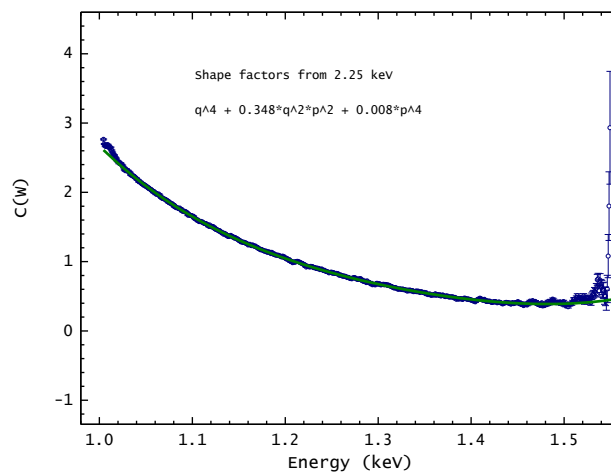


Figure 15: Rb-87 shape factor obtained by dedicated measurements enabling noise and background subtraction in the region below 12 keV.

The end point evaluation for Rb-87 led to 282.2 keV with both SSC samples available. Figure 16 reports the Kurie plot for one of the two samples. The evaluated experimental end point is in good agreement with that of

atomic mass evaluation of 282.275 keV. Using the available shape factor from Grau Carles, 2007, the present experimental data lead to an evaluation of the end point of 278.3 keV.

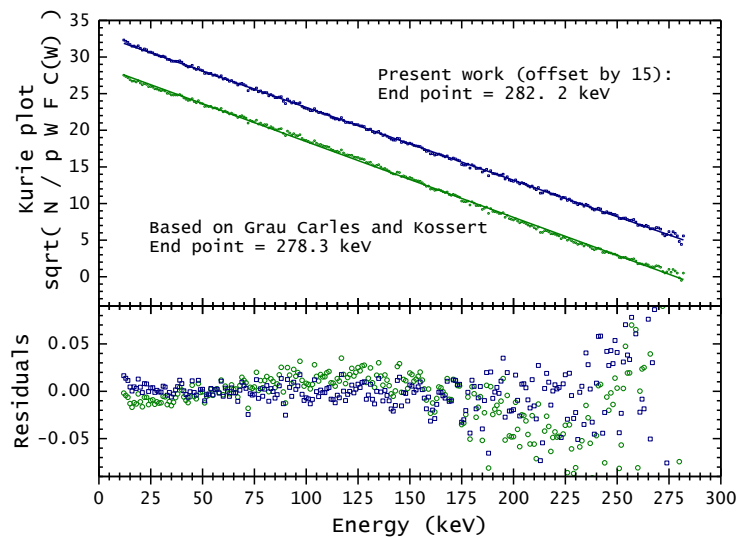


Figure 16: Kurie plot of Rb-87 and derived end points with the shape factors of Figure 13.

Beta spectra measured with a magnetic spectrometer

The magnetic spectrometer was commissioned by CHUV and a precise energy calibration was performed, prior to being used to measure the beta spectra for six radionuclides: Cl-36, Tc-99, Co-60, Cs-134, Cs-137 and Tl-204.

The main objective was to measure the beta spectra of Cl-36 and Tc-99, two 2nd non-unique forbidden transitions for which we need additional experimental data to compare with theoretical predictions. In the optimisation of the magnetic spectrometer, additional spectra were measured in order to validate the measurement set-up. Two allowed beta transitions, Co-60 and Cs-134, as well as Cs-137 a 1st unique transition, were measured. Their spectra shapes are well known and the measurements confirm the good operation of the magnetic spectrometer (Figures 19 and 20). Additionally, the spectrum of Tl-204, a known 1st unique transition, is also measured in order to compute the spectrometer efficiency energy up to 700 keV (Figure 21). The details of the magnetic spectrometer technique as well as the developments realised in the framework of the MetroBeta project are described in detail in the "Summary report on the improved measurement techniques for silicon detectors (Si(Li)), solid scintillator crystals (LaBr3/CeBr3) and magnetic spectrometers for measurements of beta spectra". All the measured spectra are presented in Figures 17 to 21. The beta spectral shapes obtained by CHUV are compared with previous measurements and/or theoretical predictions and show good agreement.

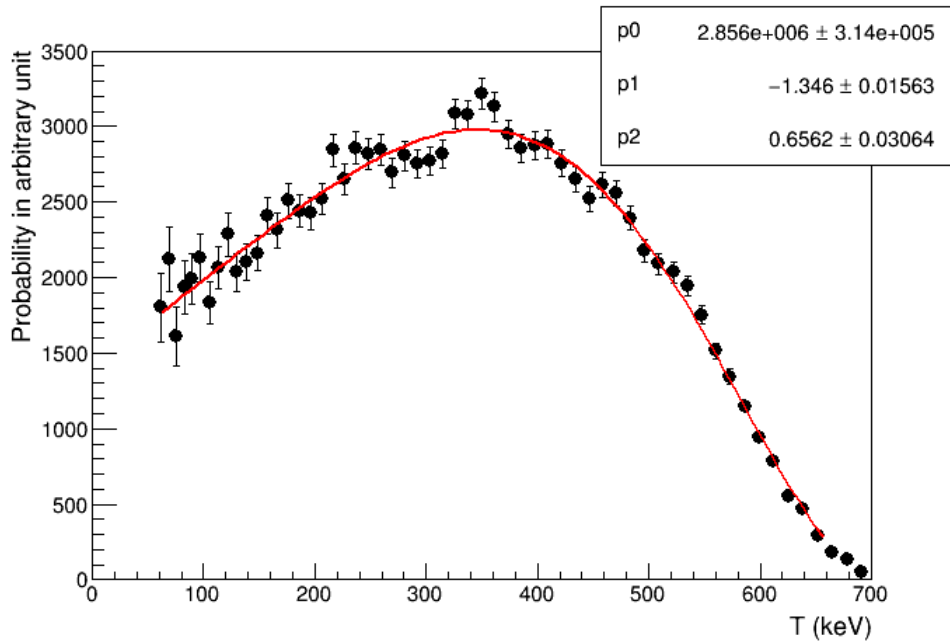


Figure 17: Measured spectrum of Cl-36. The red line gives the fit value for the a shape factor $S(W) = p_0 \cdot (1 + p_1 \cdot W + p_2 \cdot W^2)$ where W is the electron total energy, p_0 , p_1 and p_2 are fit parameters. The obtained shape factor agrees with a previous measurement from Rotzinger *et al.*, 2011.

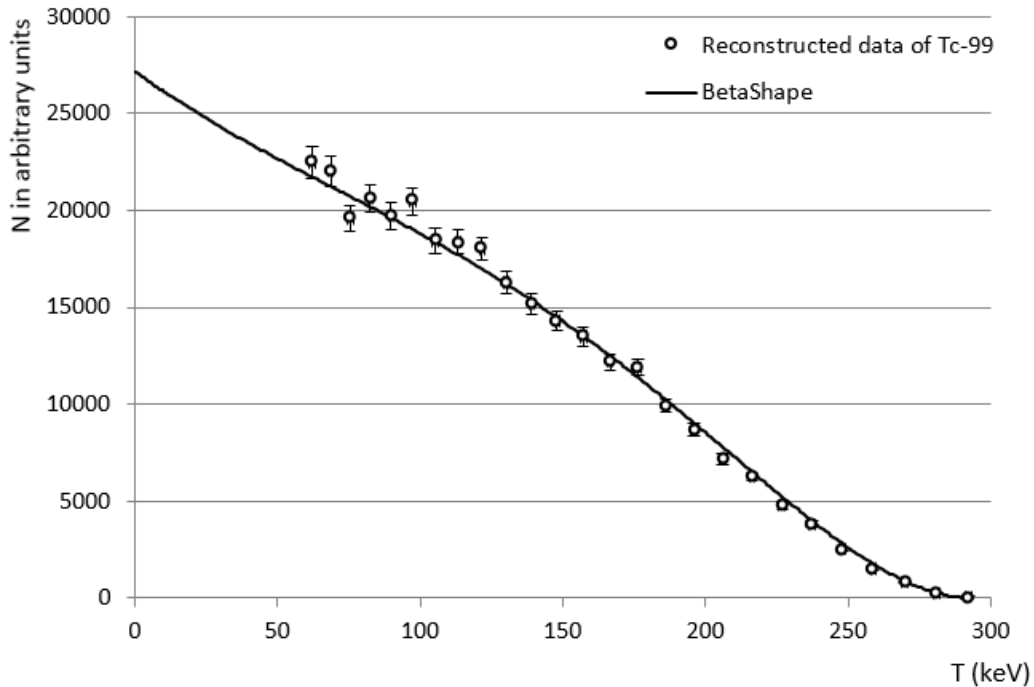


Figure 18: Measured spectrum of Tc-99. The black line corresponds to the calculated spectrum using the BetaShape code and the shape factor $S = q^2 + 0,54 \cdot p^2$ from Reich and Schüpferling, 1974, where p is the electron momentum and q the neutrino momentum.

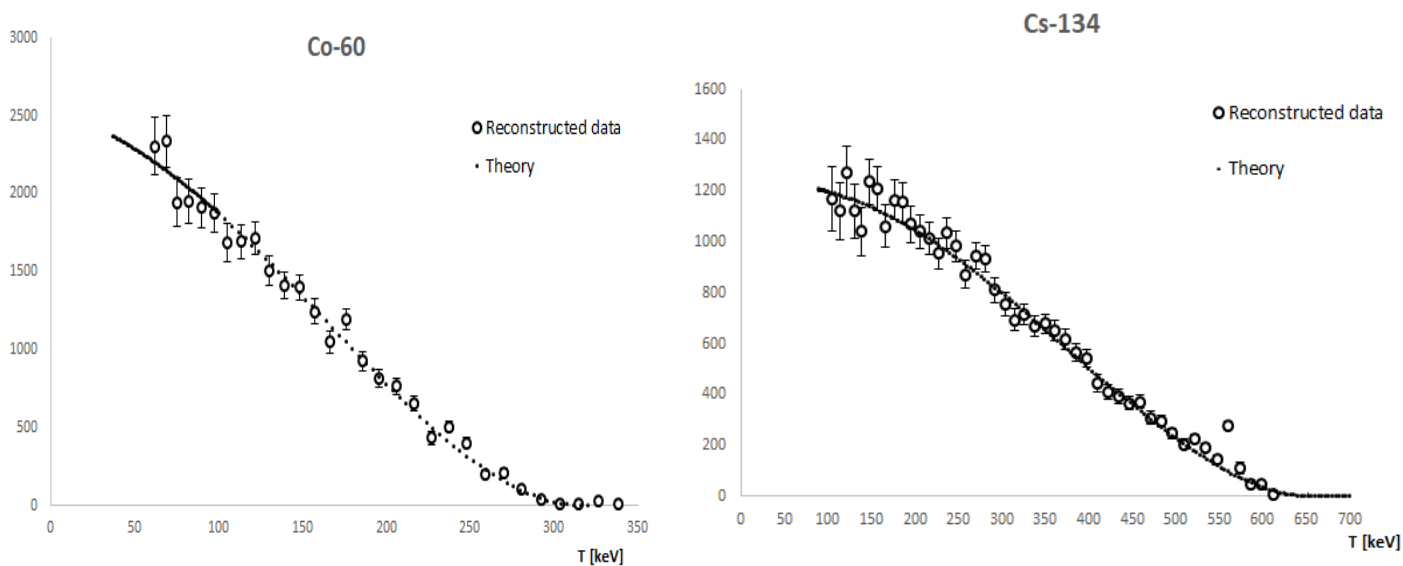


Figure 19: Measured spectrum of Co-60 and Cs-134. The black dashed line gives the expected spectrum calculated with the BetaShape code.

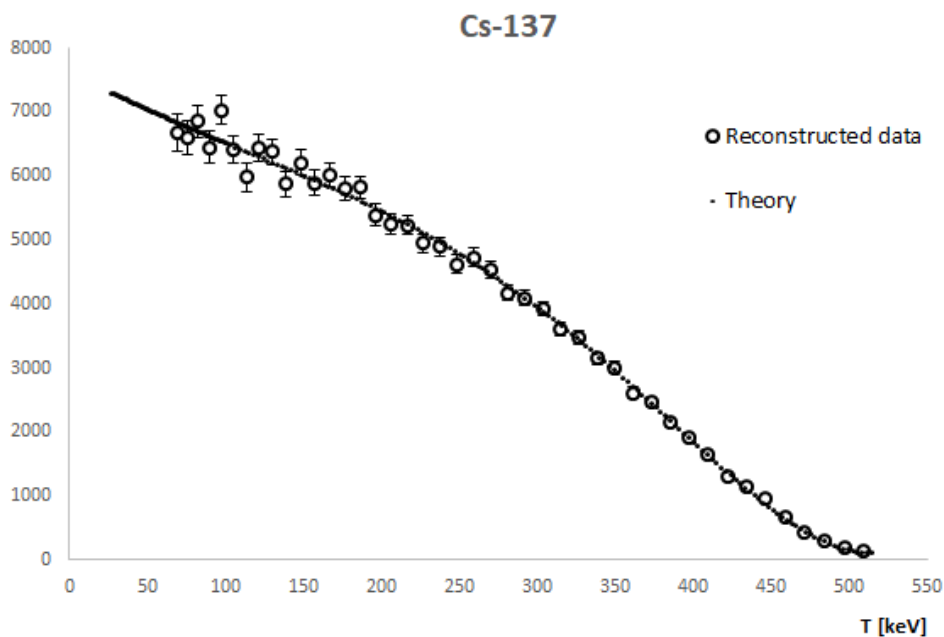


Figure 20: Measured spectrum of Cs-137. The open dot give the measurement points and the black line gives the expected spectrum calculated with the BetaShape code.

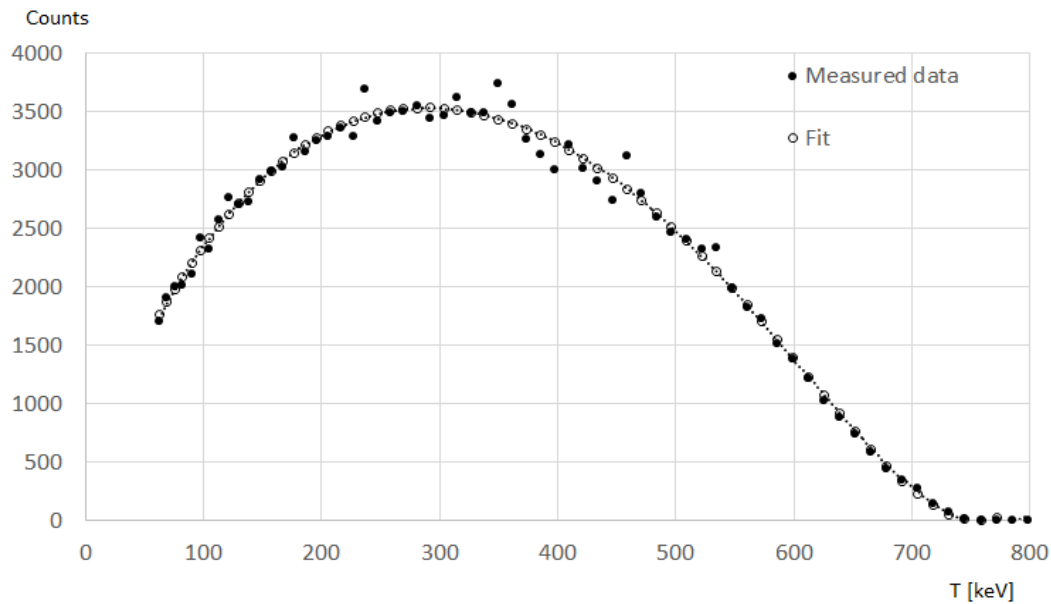


Figure 21: Measured spectrum of Tl-204. The black dots are the measured points, the dashed line with the open dots give the fit of the measured data with a sixth order polynomial.

Optimisation of beta spectrometers, based on metallic magnetic calorimeters (MMCs), and measurement of new high resolution beta spectra.

Extensive work was undertaken on the commissioning of the new metallic magnetic calorimeter based beta spectrometer by PTB, resulting in an operating device capable of measuring high resolution beta spectra. Specifically designed MMC devices were tailored to the needs for the project by UHEI and were used in the two measurement systems. Extensive development of the data acquisition system and analysis routines was carried out allowing high resolution beta spectra to be measured for four radionuclides: Sm-151, C-14, Tc-99 and Cl-36. The Sm-151 measurement also allowed an assessment to be made of the intensities of the two possible decay branches.

The development of an optimised beta spectrometer based on MMCs for these measurements is briefly summarised here. As a starting point, a set of MMC chips optimised for five different absorber heat capacities, corresponding to five different ranges of beta spectra Q values (between few keV and ~ 1 MeV), were developed and manufactured by UHEI. A dedicated UHV sputtering system, an electron beam mask writer and a dry etching system were used by UHEI for microfabrication of the MMC structures in an eight-layer process. Figure 22 presents the design of the largest (“XL”) MMC chip.

To integrate the MMCs with the signal readout SQUID, an energy calibration source and a collimator, at PTB a new detector module, shown in Figure 23 (left), has been developed. The detector-collimator distance as well as the collimator-source distance can be varied as a function of the desired count rate in the calibration photon lines. A new dilution refrigerator (Figure 23, right) was acquired and put into operation and equipped with a vibration damping system to attenuate the vibrations coupled from the pulse tube cooler into the dilution unit. At the CEA an existing detector module and dilution refrigerator (Figure 24) could be utilised.

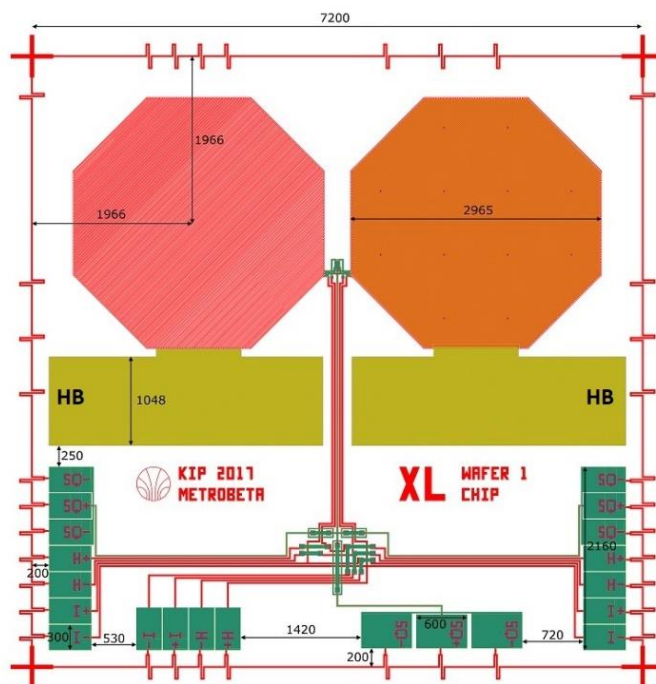


Figure 22: Layout of an MMC detector chip (type XL; HB indicate on-chip heat bath pads)

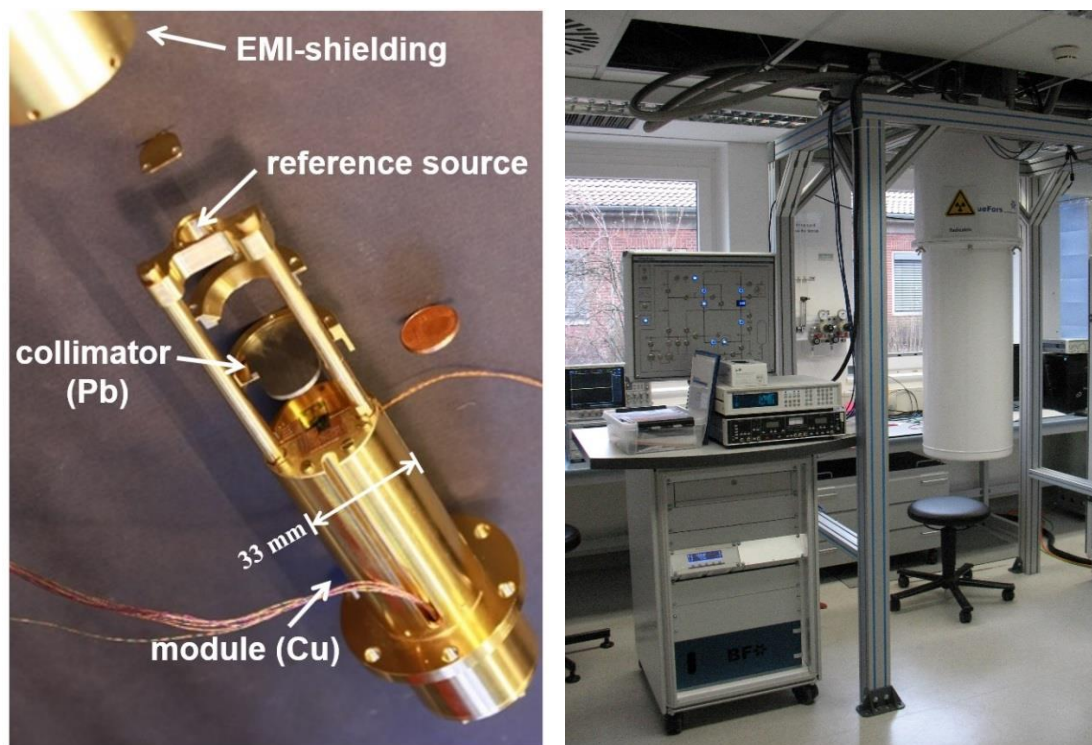


Figure 23: Left: Detector module made of gold-plated copper with collimator and a holder for an energy calibration source. Right: Dilution refrigerator at PTB

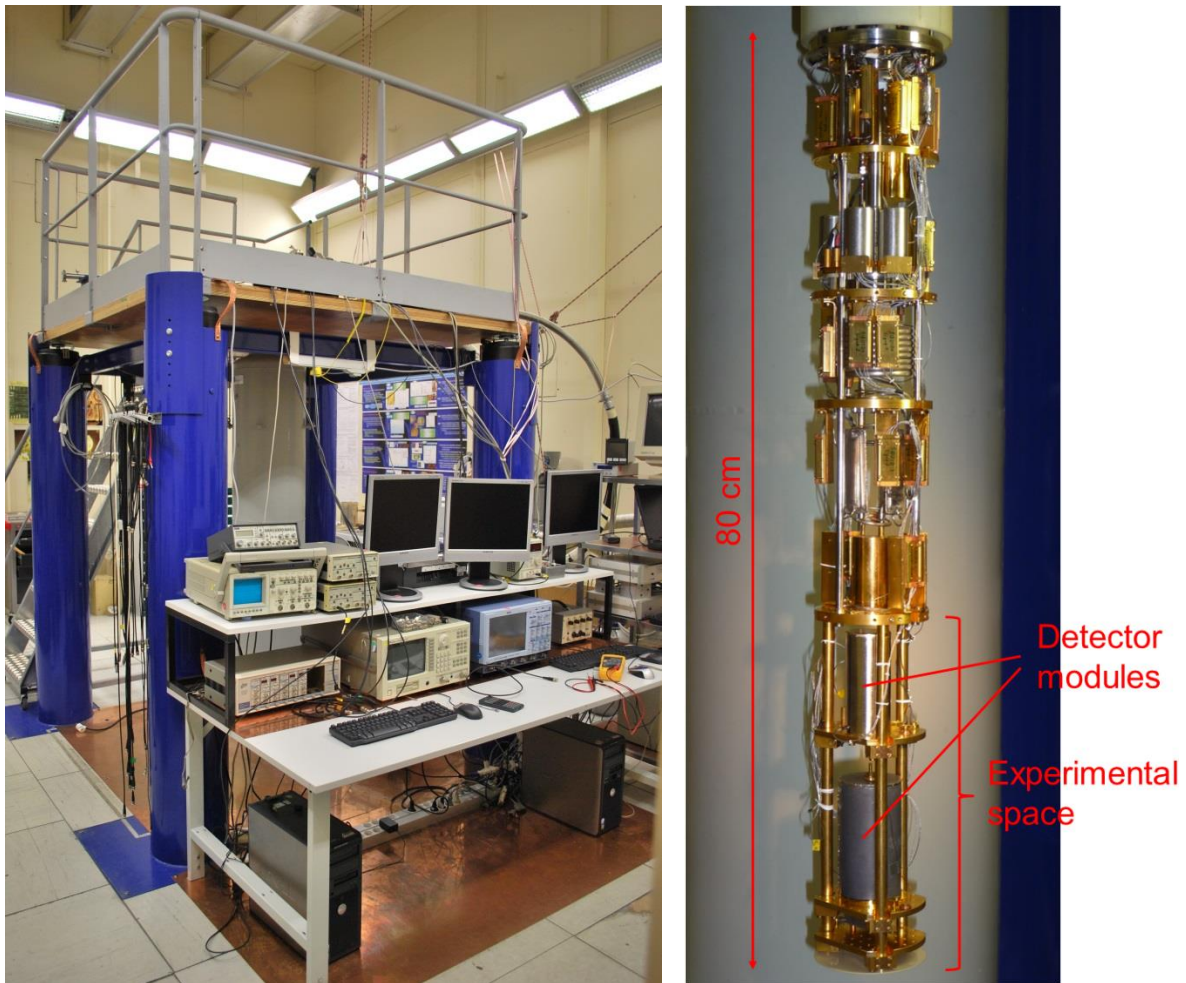


Figure 24: Left: Dilution refrigerator at LNHB. Right: Dilution unit of the dilution refrigerator. The lower third is the experimental space reaching a base temperature of 10 mK, with two detector modules installed.

The source preparation is crucial for the precise measurement of beta spectra with MMCs. The radioactive material must be completely embedded into an absorber consisting of an appropriate material to ensure that every beta particle is detected, and the entire energy is deposited and thermalized, i.e. transformed to heat. Within the framework of this project, the radioactive material was deposited by two different methods, electrodeposition as well as drop deposition, either directly onto the absorber material or onto a separate source carrier foil. To enclose the sources inside the absorber and realize a 4π geometry, in the first case a second foil of absorber material was placed on top of the first foil with the source, in the second case the source carrier foil was sandwiched between bottom and top absorber foils. Each stack of foils was then bonded together by diffusion welding. Temperature, pressure and processing time were varied to fabricate the 4π source/absorber assemblies. The parameters to obtain reliable enclosure were found to depend strongly on the absorber material as well as on the radionuclide and the chemical composition of the source material.

The best source preparation approach - besides implanting the radionuclide directly into the absorber material - is a metallic layer formed by electrodeposition, as long as this is possible for the considered element. In many cases, an oxide/hydroxide layer will form during electrodeposition. This can still be a good quality source consisting in a very thin, homogenous layer. In the past, some experience has been gained with electrodeposition of beta emitters for MMC-based measurements, forming both metal (^{63}Ni) and oxide/hydroxide (^{241}Pu) layers. Within this project, a ^{151}Sm source was electrodeposited on a silver foil, forming a Sm oxide/hydroxide layer. Also ^{99}Tc was electrodeposited; the deposit is barely visible but, according to the adopted electrodeposition procedure, should be metallic technetium.

Where electrodeposition is not possible, as in the case of ^{14}C or ^{36}Cl , drop-deposited sources were produced. Typical radionuclide solutions contain certain salt loads, which means that drop deposition often leads to the formation of large (of the order of micrometers) salt crystals. Previous studies have revealed that salt crystals can cause considerable spectrum distortion due to incomplete thermalisation. One approach to avoid the formation of large salt crystals is to decrease the individual drop size to a few picolitres, and to deposit a number of droplets corresponding to the required activity in a 2D-array pattern. Commercial micro-dispensing systems can deposit single droplet volumes of less than 50 μl in combination with a placement accuracy of better than 20 μm . With the help of an automated micro-dispensing system different radionuclide solutions (^{36}Cl , ^{99}Tc , and ^{14}C) were deposited onto gold foils. Milling techniques were used to format gold foils into an array of absorber elements with lateral dimensions of about 0.7 mm and 1.6 mm. Figure 25 a) shows an absorber array after the radioactive solution was dried. Here, volumes of 100 nl (left half) and 50 nl (right half) of a ^{99}Tc solution were deposited in the middle of each marked absorber. The fact that the deposit is not visible indicates the absence of large crystallizations. Checking the activity by visual inspection is hence not possible but based on the results of an autoradiographic image, see Figure 25 b), the positions and the different activities of the deposited material were confirmed. The quality of a drop-deposited source, prepared with a micro-dispensing system, can be demonstrated by comparing its measured spectrum with that of an electroplated source.

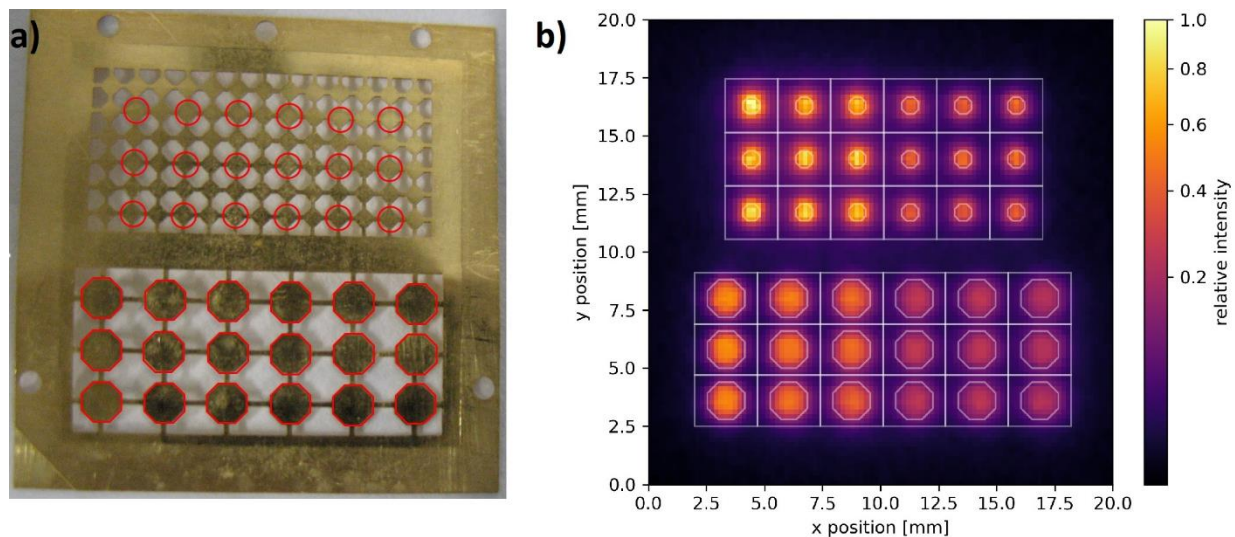


Figure 25: **a)** Photograph of an array of pre-fabricated gold absorber foils with ^{99}Tc sources deposited by a microdrop dispenser system in the middle of the marked absorbers. **b)** Autoradiographic image of the same array. Two different activities, 5 Bq / 2.5 Bq, have been deposited on each marked absorber in the left / right half of the array. The activity is well centred on each absorber.

Fine dispersion of the source material in the absorber metal will also improve the source quality compared to a conventional drop-deposited source. One technique resulting in fine dispersion consists in alternate folding and laminating of the foil with the source deposit. This breaks the source crystals into tens of nanometre small particles that are embedded in the metal foil. Since, after this mechanical processing, the activity is dispersed in the entire foil volume, this source foil must then be sandwiched between two metal foils of the required thickness. This technique was applied to the electrodeposited ^{151}Sm source, because its layer was blackish and was considered not to be ideally thin. Another technique resulting in fine dispersion consists in the absorption of radionuclide solutions into nano-porous metal samples. In the context of Q spectroscopy of alpha emitters, deposition of actinide solutions into gold nanofoam, constraining the crystals to the pore size of tens of nanometres, is also being studied. The gold nanofoam has been prepared by de-alloying a gold-silver alloy with phosphoric acid. The pore size can be controlled via the concentration and the temperature of the etchant and the etching time.

Novel bilayer absorbers are being developed, in order to measure the beta spectrum of ^{36}Cl ($Q = 709.53$ keV) which suffers from distortion due to bremsstrahlung escape when pure gold absorbers are employed. The distortions are reduced by embedding the radionuclide into 2×150 μm copper foils ($Z = 29$) and adding additional 2×200 μm gold foils ($Z = 79$) around the copper. While the copper layers lead to less

Bremsstrahlung generation and reduce the energy of the emitted beta particles, the high stopping power of the surrounding gold layers fully stops the electrons while keeping the overall absorber dimensions and the related heat capacity small. Preparing this kind of absorber requires several steps of diffusion welding in an oxygen-free oven to avoid the oxidation of the copper.

Beta spectra measured with optimised metallic magnetic calorimeters

Four beta spectra have been measured using MMCs within the MetroBeta project, although in the challenging measurement of the spectrum of ^{36}Cl the experimental conditions were not optimal, leading to a degraded energy resolution. New measurements under improved conditions are under preparation.

^{14}C

The spectrum of ^{14}C has been measured using a source prepared by conventional drop deposition, but from a carrier-free, high specific activity solution. After drying, the deposit was invisible, even under an optical microscope, so the source can be considered to be of high quality. It was deposited on a 25 μm thick gold foil, thick enough to stop all beta particles up to the end point of the spectrum (156.5 keV). Since the ^{14}C atoms are bound in a volatile organic compound, diffusion welding is not a viable option for source enclosure. The foil with the source was just folded over and slightly pressed. Gold is highly ductile and keeps its shape once folded; no beta electrons can escape from being absorbed in the gold absorber. Gold is a good thermal conductor at very low temperature, so the thermal contact between the two halves of the absorber through the bending is sufficient. The absorber (Au , 1 $\text{mm}^2 \times (2 \times 25 \mu\text{m})$) was placed on an MMC chip whose size best matches its heat capacity ($C_{\text{abs}} = 67 \text{ pJ/K}$ at 20 mK). The experimental conditions during the spectrum measurement were far from optimal. During the cooling phase, the glue layer fixing the MMC chip to its holder broke, the chip was then only suspended by the gold and aluminum bonding wires used for electrical and thermal contacts. This had two consequences degrading the detector performance. One of them is that the thermal time constant of the detector was longer than expected, leading to a large fraction – more than 50 % – of piled-up pulses that had to be removed from the data set. The major part of pile-up is removed by applying an extendable dead-time. A cut on the chi-square of the optimal filter used for the pulse-height determination removes practically all remaining piled-up events, too closely spaced in time to be detected separately and removed by the dead-time. The chi-square criterion is a measure for deviations of the pulse shape from the normal one. After 10 days of data acquisition at a rate of ~ 7 counts per second, the final spectrum, shown in Figure 26, contains 2.7 million events.

The lines at 22 keV, 25 keV and 88 keV are K X-ray and gamma ray lines from an external ^{109}Cd source and the broad line at around 6 keV, in reality a clipped double line, is the $K\alpha + \beta$ line of an external ^{55}Fe source; these lines are used for energy calibration. The weak lines at around 10 keV are escape lines.) The increase of the spectrum below 6 keV may be due to the degraded detector performance; a new measurement under improved conditions should clarify this question.

The other consequence is that the MMC could vibrate, resulting in an energy resolution near 200 eV (FWHM), about a factor 5 worse than expected from the absorber heat capacity. Nevertheless, the detector performance was much better than another published measurement. The energy resolution was improved by a factor five, while the energy threshold was reduced from ~ 5 keV to ~ 700 eV.

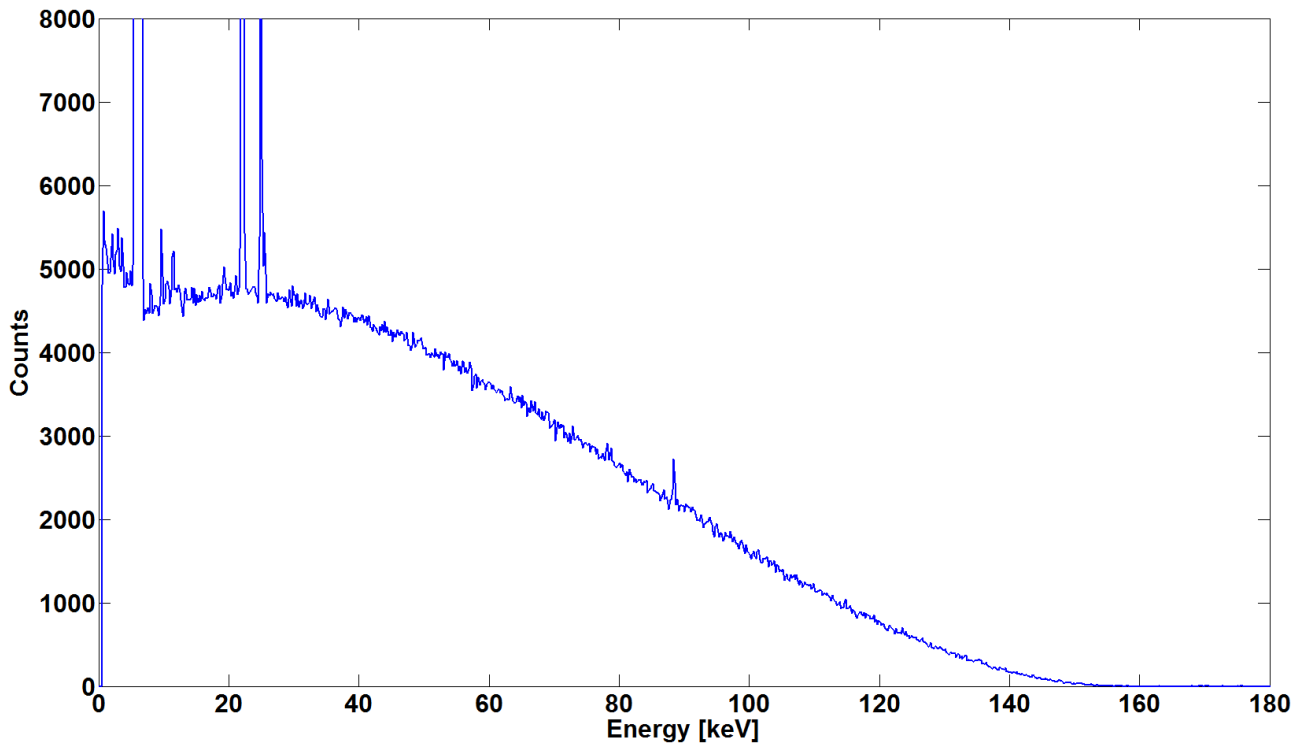


Figure 26: Beta spectrum of ^{14}C measured with an MMC.

^{151}Sm

A ^{151}Sm source was electrodeposited on a $10\ \mu\text{m}$ thick silver foil. After the mechanical processing, this source foil ($0.8\ \text{mm} \times 0.8\ \text{mm} \times 7\ \mu\text{m}$) was sandwiched between two silver foils ($0.9\ \text{mm} \times 0.9\ \text{mm} \times 15\ \mu\text{m}$ each) and the three foils were diffusion-welded to form the absorber (heat capacity: $29\ \text{pJ/K}$ at $20\ \text{mK}$). The performance of the MMC during this measurement was as expected. An energy resolution ranging from about $45\ \text{eV}$ (FWHM) at $6\ \text{keV}$ to $70\ \text{eV}$ at $25\ \text{keV}$ and an energy threshold of $250\ \text{eV}$ were observed. It should be mentioned here that under optimal conditions the energy resolution of an MMC is nearly independent of energy since it is only limited by noise. Various effects like temperature fluctuation of the thermal bath can, however, introduce some energy-dependent terms. The thermal time constant ($1/e$) of the detector was $460\ \mu\text{s}$; at a count rate of $8.7\ \text{s}^{-1}$, the fraction of piled-up pulses was very low. After 14 days of data acquisition, the spectrum contains 10.2 million events after pile-up suppression.

Sm-151 is the only non-pure beta emitter measured within the MetroBeta project: It has a main β^- decay branch ($Q_\beta = 76.3\ \text{keV}$) to the ground state and a second β^- decay branch to the $21.54\ \text{keV}$ excited level of ^{151}Eu . Both transitions are first forbidden non-unique. The DDEP recommended values for the respective probabilities of the two decay paths are $99.07(4)\%$ and $0.93(4)\%$. The de-excitation of the $21.54\ \text{keV}$ excited state is highly converted; only 3.4% of the gamma transition leads to the emission of gamma-rays (total probability: $3.24(13) \times 10^{-4}$), the remainder leads to the emission of conversion electrons and subsequently X-rays and/or Auger electrons. The detector absorber with its given dimensions, sufficient to stop all beta electrons up to the beta Q value, also stops all conversion electrons, more than 99% of all X-rays and more than 95% of the $21.54\ \text{keV}$ gamma photons. The result is that for practically all beta decays to the excited level the sum of the beta energy and the gamma energy is absorbed. So the measured spectrum for the decays to the excited level is shifted by the energy of the gamma transition and starts at $21.54\ \text{keV}$, leading to a step in the recorded spectrum. Since the maximum energy for this beta branch equals the Q value minus the gamma transition energy, the end point of both measured spectra is the same, $76.3\ \text{keV}$. As it is not possible to distinguish events from the two decay branches, both spectra are superimposed in one experimental spectrum.

The measured spectrum is shown in Figure 27 together with theoretical spectra calculated with the code BetaShape for both decay paths. The spectrum corresponding to the decay to the ground state was fitted to the experimental spectrum in the energy range from $10\ \text{keV}$ to $20\ \text{keV}$. It can clearly be seen that above

21.5 keV the experimental spectrum lies higher than the fitted spectrum of the main decay branch. The spectrum corresponding to the decay to the excited level was shifted by 21.54 keV and fitted to the experimental spectrum in the energy range 26 keV – 40 keV. The area lying between the two theoretical spectra, corresponding to the probability of the decay to the excited state of ^{151}Eu , amounts to 2.6 % of the total. We do not state any uncertainty on the measured probability, firstly because the theoretical spectra are preliminary, secondly because the theoretical spectrum does not fit the experimental spectrum below 6 keV, and thirdly because the fitting procedure was rather coarse. Nevertheless, this value is in clear contradiction with the recommended value of 0.93(4) % for the probability of the decay to the ^{151}Eu excited level. Concerning the beta spectrum shape, the discrepancy between experiment and theory at low energies is most likely due to an incomplete control of the atomic effects in the theoretical calculation of this first forbidden, non-unique transition.

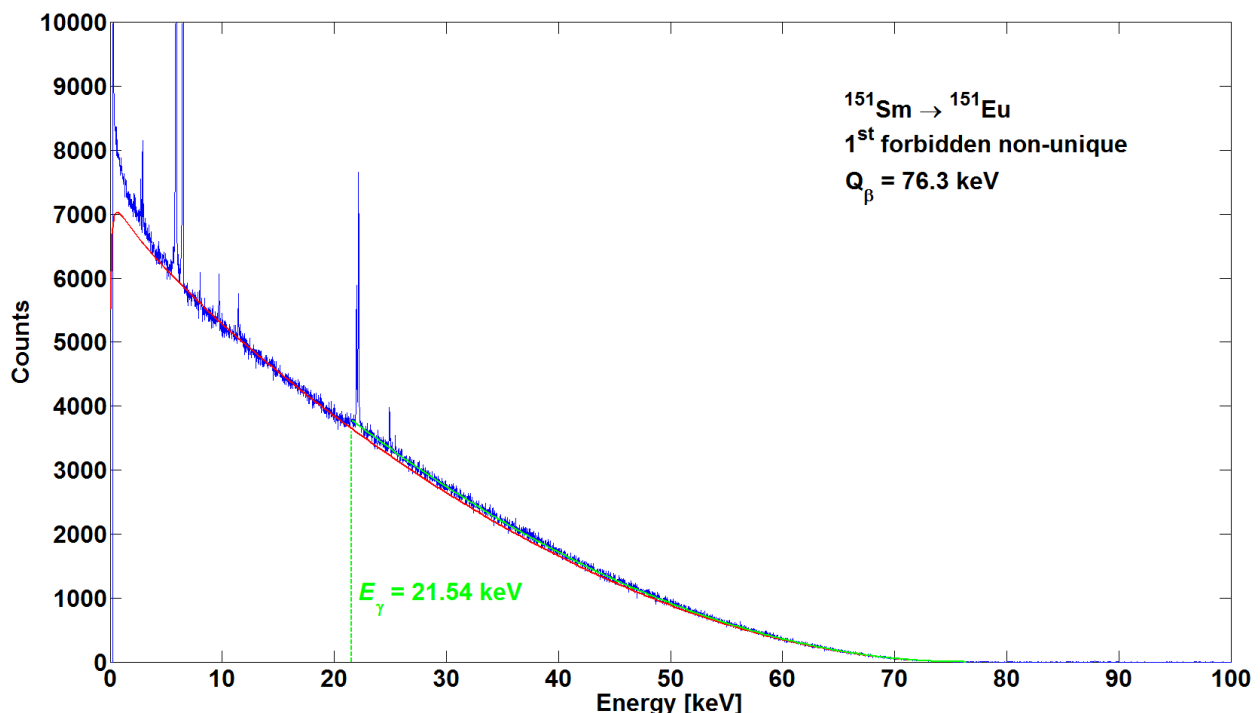


Figure 27: Beta spectrum of ^{151}Sm measured with an MMC (blue) together with theoretical spectra calculated for the two beta decay branches, to the ground state (red) and to the 21.54 keV excited level of ^{151}Eu (green).

The spectrum from the transition to the excited state is shifted towards higher energies by 21.54 keV, the energy of the gamma transition that is detected in sum with the beta particle energy.

Therefore both measured spectra end at the same energy, 76.3 keV.

The energy calibration was performed with an external X-ray source composed of ^{55}Fe and ^{109}Cd .

^{36}Cl

A ^{36}Cl source has been fabricated by means of the micro-drop dispenser directly on a 300 μm thick gold foil formatted to an array of absorber elements with lateral dimensions of about 1.6 mm and 0.7 mm, like the one shown in Figure 25 a). An identical foil was diffusion welded onto the first foil with the dried radioactive material. One of the 1.6 mm-absorbers (heat capacity at the detector operating temperature, i. e. 20 mK: 1.8 nJ/K) was glued to one of the sensors of an XL MMC-chip, very well matched to the absorber heat capacity (optimized for 1.7 nJ/K). An external ^{241}Am source was added to the setup and the photons were collimated onto the gold absorber for energy calibration. The setup was mounted in the PTB dilution refrigerator; data was acquired at 20 mK during 140 hours. After data analysis including several cuts, the final spectrum, shown in Figure 28, contains 750 000 events.

This measurement suffered from two problems. Firstly, the pulse time constants were much longer than intended. This can be explained by the new chip design, whose behaviour was not yet well enough known at the date of the measurement, and by the heat capacity of the absorber that is extremely large for a cryogenic detector. The time constants can, however, be adjusted in future measurements. Secondly, the vibrations of

the pulse tube providing the cooling power at 3.5 K produced a parasitic signal with an amplitude several times larger than the pulse height of the beta decay events in the detector. This degraded the energy resolution to ~ 3.8 keV at the 59.54 keV ^{241}Am gamma ray line. Since this experiment the strong vibrations could be very efficiently damped at the detector level by a spring suspension of the detector support plate. This led to a significant improvement of the energy resolution as will be seen in the following section on the ^{99}Tc beta spectrum.

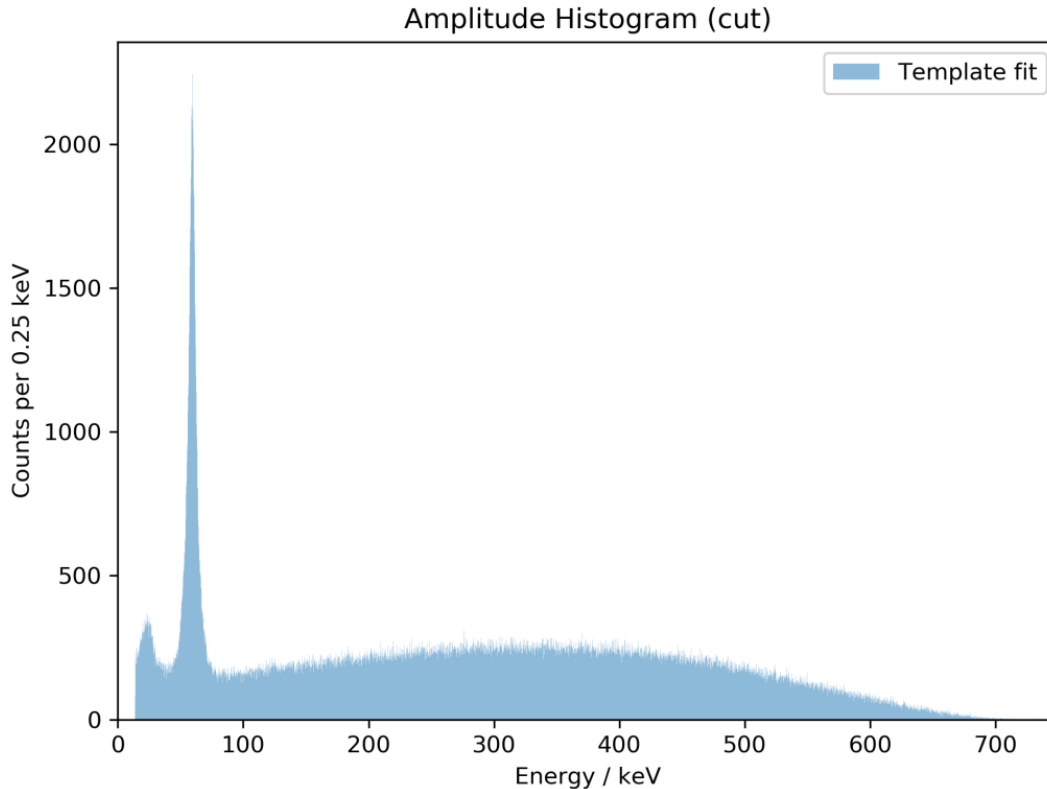


Figure 28: Beta spectrum of ^{36}Cl measured with an MMC. Energy calibration was performed using the gamma-ray photons from an external ^{241}Am source.

^{99}Tc

The beta spectrum of ^{99}Tc was measured both at PTB and at CEA. What makes this comparison interesting is that these measurements are completely independent. The technetium sources were prepared by different techniques and are of different chemical composition. The MMCs were mounted in different detector modules. The measurements used different cryogenic setups in different electromagnetic environments. Data were recorded by different data acquisition systems, and data analysis was performed using different routines.

At CEA, a ^{99}Tc source was electrodeposited on a 10 μm thick gold foil. The deposit is extremely thin and should be metallic technetium. However, the deposition yield and the resulting activity per surface area were lower than expected. Therefore a sufficiently large piece of this foil had to be folded three times to reduce its area to a size (~ 0.5 mm \times 0.7 mm) small enough to enclose it in an MMC absorber. This source foil was then sandwiched between two gold foils (0.9 mm \times 0.9 mm \times 74 μm each) and this stack was diffusion welded. The final absorber had a heat capacity of 350 pJ/K at 20 mK, much larger than the previous detectors. The pulses had a rise time (10 % - 90 %) of 14 μs and a decay time (1/e) of 2.15 ms. Data were acquired during 13.7 days and the spectrum contains 5.65 million events. The energy resolution is practically energy-independent, about 100 eV (FWHM) up to 384 keV, the highest energy gamma line of a ^{133}Ba source used for energy calibration and check of the linearity. Comparing the measured and the tabulated line energies between 31 keV and 384 keV shows no larger deviations than 70 eV, less than the energy resolution, and no obvious trend.

At PTB, a ^{99}Tc source was prepared with a micro-drop dispenser directly on a 90 μm thick gold foil formatted to an array of absorber elements with lateral dimensions of about 1.6 mm and 0.7 mm. An identical foil was diffusion welded onto the first foil with the dried radioactive material. One of the larger source/absorber assemblies with an expected activity of about 5 Bq was selected and glued onto a matching MMC. The heat capacity of the absorber assembly is 545 $\mu\text{J/K}$ at 20 mK. The observed pulses had a rise time (10 % - 90 %) of 31 μs and a decay time (1/e) of 4.6 ms. The data acquisition took 42 h and the resulting spectrum consisted of 0.5 million events with an energy threshold of about 5 keV. A ^{57}Co source was used for energy calibration and the 122 keV gamma line showed an energy resolution of 600 eV (FWHM). The larger absorber and total heat capacity of the setup, as well as experimental problems with the temperature stability of the thermal bath explain the degraded energy resolution and threshold compared to the measurement performed at CEA.

Figure 29 shows a superposition of both experimental spectra. It is clear that the spectrum shape is practically the same. As in the case of ^{36}Cl , this spectrum shape will be a valuable input for the improvement of the theoretical calculation for this type of transition, 2nd forbidden non-unique. It is noteworthy that the spectrum measured at CEA (labelled LNHB) has an energy threshold of 650 eV, practically two orders of magnitude lower than any spectrum published to date.

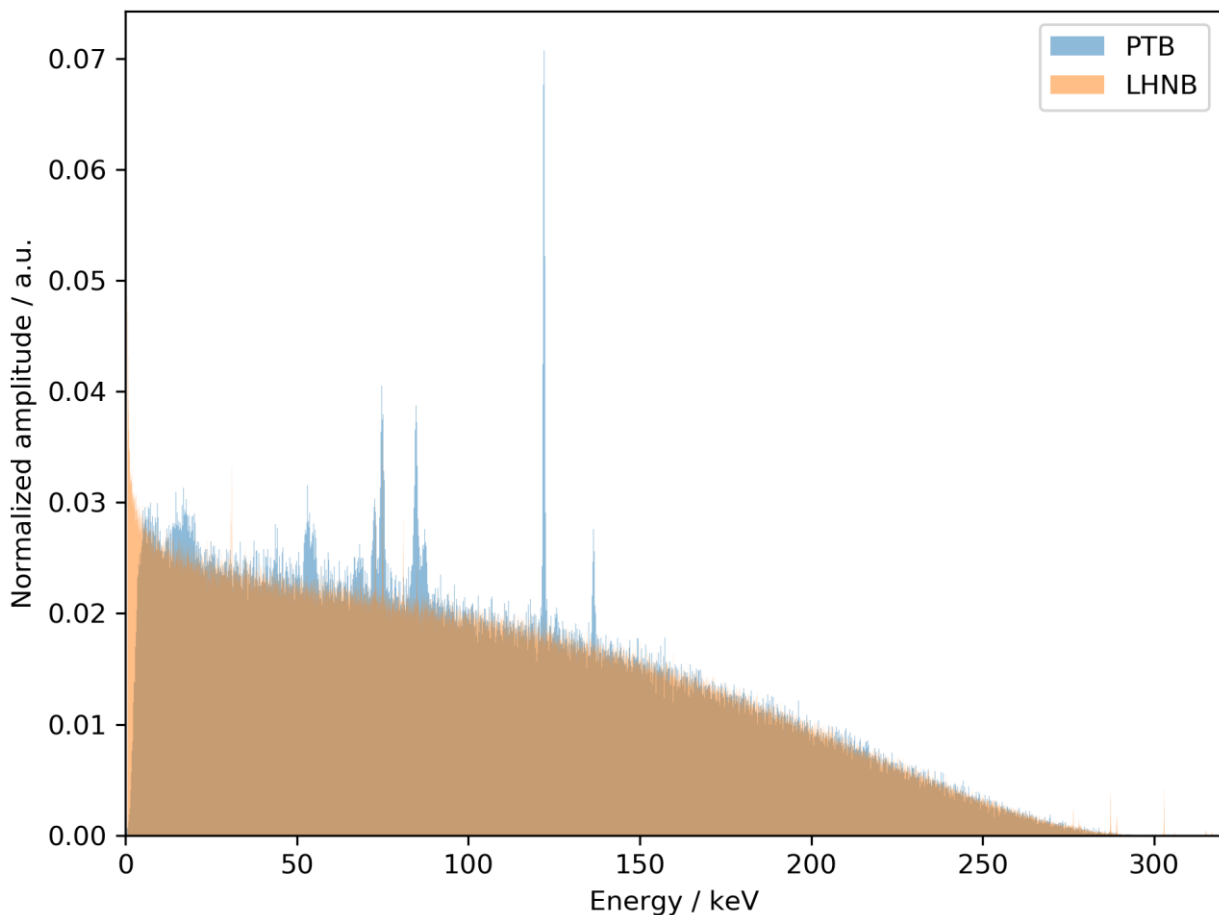


Figure 29: Beta spectrum of ^{99}Tc measured with sources fabricated in two different ways, with two independent MMCs, in different setups and using different data analysis routines. The energy calibration was performed with a ^{133}Ba source at CEA (LNHB) and a ^{57}Co source at PTB.

Improvement of theoretical methods on the basis of the measured spectra and comparison of the measured and calculated beta spectra.

The code, BetaShape, used for the calculation of theoretical beta spectra was further developed and tested by CEA and UMCS. A simplified model to determine the nucleon wave functions using either a relativistic or non-relativistic harmonic oscillator was included, as well as a phenomenological nuclear mean-field approach employing the so-called Woods-Saxon potential developed by UMCS. The intrinsic model in the code was re-implemented during this project owing to inconsistencies seen through the coupling with the nuclear structure component. The propagation of the uncertainties in the calculation of the nuclear structure components has now been included into the relevant part of the calculations. The new parameterisation of the Woods-Saxon potential of the mean-field Hamiltonian and the spin-orbital potential was used by UMCS to generate the realistic nucleonic wave-functions for calculating the beta spectra. A number of peer-reviewed articles have been published by CEA and UMCS giving details on the calculations.

Figure 27 has already shown the comparison of the theoretical spectrum calculated with the BetaShape code with the spectrum of ^{151}Sm measured using the optimised metallic magnetic calorimeters, and illustrates the possibility to determine the branching fraction for the two beta transitions.

Figure 30 shows the theoretical spectrum compared to the measured spectrum for ^{14}C .

The lines at 22 keV, 25 keV and 88 keV are K X-ray and gamma ray lines from an external ^{109}Cd source and the broad line at around 6 keV, in reality a clipped double line, is the $K\alpha + \beta$ line of an external ^{55}Fe source; these lines are used for energy calibration. The weak lines at around 10 keV are escape lines. The red line is the theoretical spectrum. The increase of the experimental spectrum at low energies and deviation from the theoretical curve may be due to the degraded detector performance; a new measurement under improved conditions would be able to clarify this question.

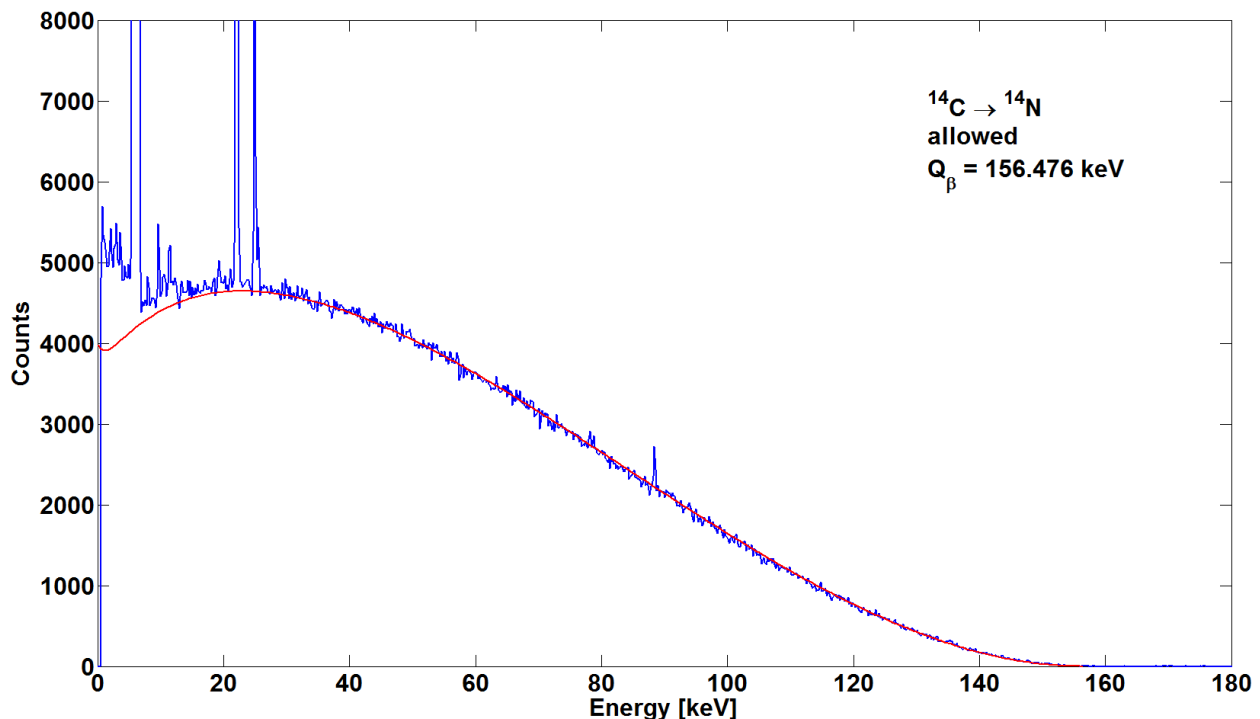


Figure 30: Beta spectrum of ^{14}C measured with an MMC (blue) and the theoretical spectrum calculated with the BetaShape code (red).

The beta spectrum of ^{99}Tc was measured both at PTB and at CEA and is shown in Figure 31, along with the theoretical spectrum calculated with the BetaShape code. What makes this comparison interesting is that these measurements are completely independent. The technetium sources were prepared by different techniques and are of different chemical composition. The MMCs were mounted in different detector modules. The

measurements used different cryogenic setups in different electromagnetic environments. Data were recorded by different data acquisition systems, and data analysis was performed using different routines.

Figure 31 shows a superposition of both experimental spectra. It is clear that the spectrum shape is practically the same. As in the case of ^{36}Cl , this spectrum shape will be a valuable input for the improvement of the theoretical calculation for this type of transition, 2nd forbidden non-unique. The theoretical spectrum that is also shown in Figure 31 has been calculated with the current version of the code BetaShape, supposing an allowed transition, and multiplied with an experimental shape factor. It is not surprising that this shape factor, derived from a measurement with an energy threshold at 55 keV, cannot correctly reproduce the spectrum at lower energies. It is noteworthy that the spectrum measured at CEA has an energy threshold of 650 eV, practically two orders of magnitude lower than any spectrum published to date.

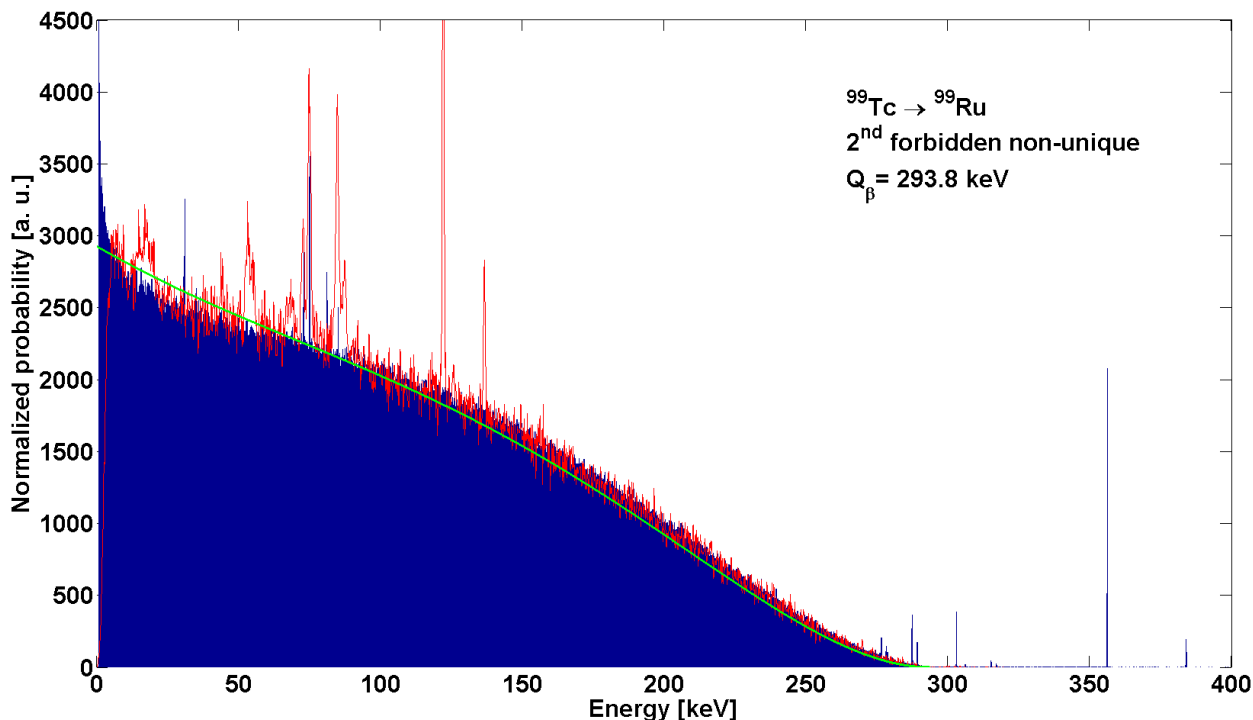


Figure 31: Beta spectrum of ^{99}Tc measured with ^{99}Tc sources fabricated in two different ways, with two independent MMCs, in different setups and using different data analysis routines. For better visibility, one spectrum is represented as a histogram (blue, measured at CEA) and the other one as a line (red, measured at PTB). The energy calibration was performed with a ^{133}Ba source (CEA) respectively a ^{57}Co source (PTB). The theoretical spectrum calculated with the BetaShape code is also shown (green).

Investigation of the effect of improved beta spectra on absolute activity measurements and measurement of Bremsstrahlung production.

Effect of improved beta spectra on absolute activity measurements

Comprehensive studies were made on the absolute activity determination of ^{60}Co and ^{99}Tc using two primary activity measurement methods, based on liquid scintillation counting. Results have already been published for ^{60}Co , and they underline the importance of using accurate beta spectra. Further studies were carried out using the TDCR-Cerenkov technique for ^{36}Cl . These studies have been reported in full detail.

The study of ^{63}Ni was already presented prior to the MetroBeta project, but some important aspects are summarised since these are important to understand the concept of beta spectrum validation by means of LSC. In addition, the example demonstrates the importance of beta spectra and, thus, it is a key motivation for this EMPIR project.

Nickel-63 is a pure beta emitter with an allowed transition and a maximum energy of about 67 keV. Hence, the above-mentioned LSC methods are well suited for activity standardization.

The analysis of experimental data obtained from TDCR and CNET, however, revealed discrepancies when using beta spectrum calculation as used in common LSC efficiency calculation tools (Figure 32). In the following, we call the spectrum from such a calculation the classical beta spectrum, which means, that screening corrections and the atomic exchange effect are not taken into account. Figure 33 shows two important phenomena when using this classical beta spectrum:

There is a trend in the CNET data when varying the counting efficiency. The results of CNET and TDCR do not agree. The discrepancies cannot be explained with a choice of the kB parameter for the ionization quenching. Here, $kB = 0.0075$ cm/MeV was used.

The situation only improved when using a more realistic approach for the beta spectrum calculation which accounts for screening and atomic exchange effect. In this case, no significant trend was found for both methods and the results of TDCR and CNET are in agreement. The two different beta spectra are shown in Figure 32. The results for the determined activity concentration with both parameterisations are shown in Figure 33. It must also be emphasised that there is a significant change in the mean activity concentration which demonstrates the importance of the beta spectrum. It should be noted that the improved calculation method is strongly supported by the previously experimentally determined beta spectrum using MMCs.

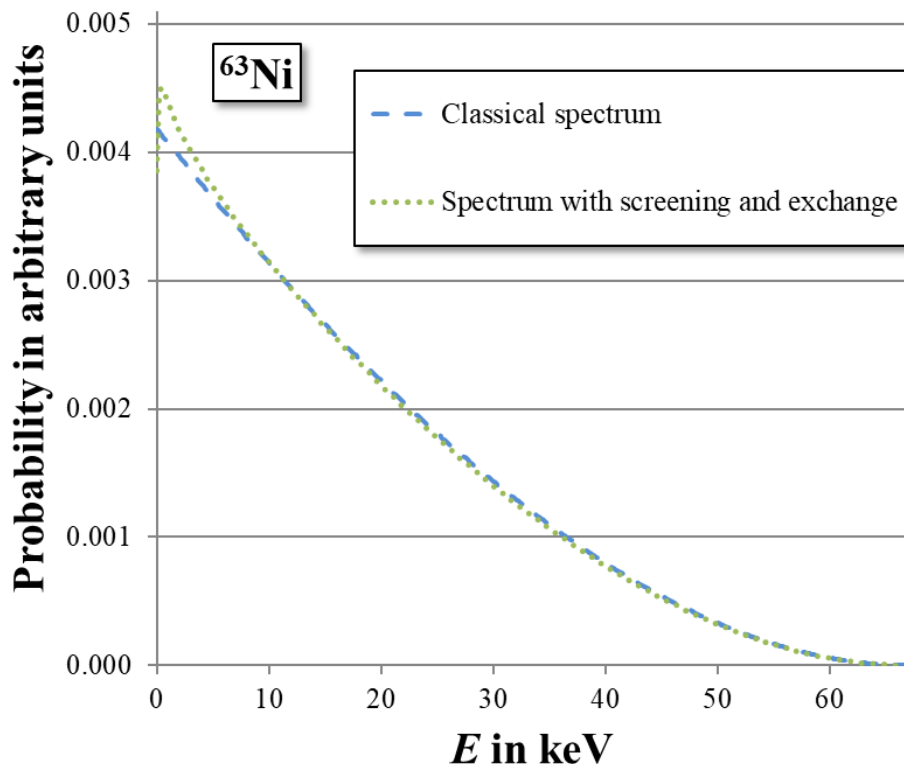


Figure 32: Computed beta spectra for ^{63}Ni . The classical spectrum was calculated without any correction whilst the screening correction and the exchange effect were taken into account for the other spectrum by using the BetaShape code.

The outcome when using another beta spectrum calculation was also analysed and interestingly, this also led to agreement between both the TDCR and CNET methods, without any significant trend when varying the efficiency, but the activity concentration was found to be higher. This shows that there are limitations of the validation method which, in this case, cannot judge which of the parameterisation is better (more realistic). Hence, it would be desirable to study a radionuclide, for which the activity can be determined independently without any knowledge about the beta spectrum. This was achieved by studying ^{60}Co as described below.

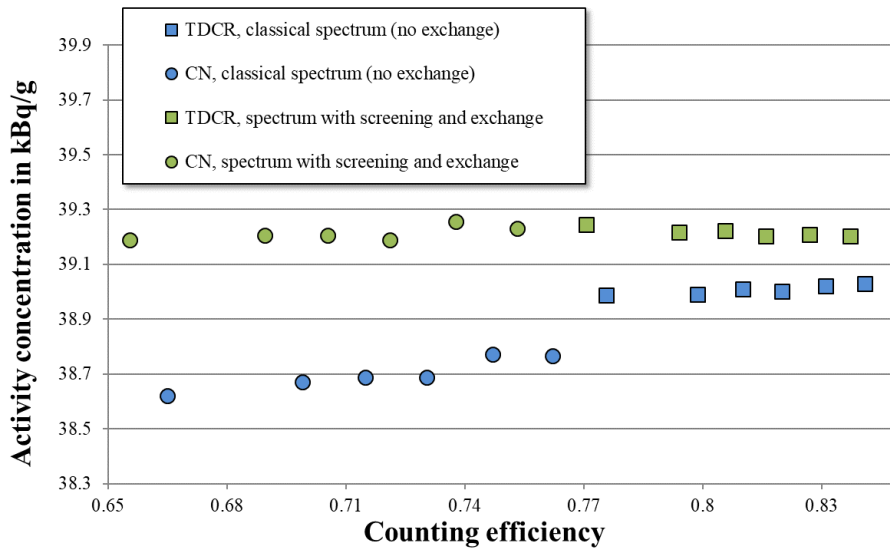


Figure 33: Activity concentration of the ^{63}Ni solution as a function of the ^{63}Ni counting efficiency when using a kB parameter of 0.0075 cm/MeV.

The beta decay of ^{60}Co is accompanied with gamma-ray transitions. Hence, this radionuclide is usually standardised by means of coincidence counting techniques. Within the MetroBeta project, a solution was measured by means of two $4\pi\beta\text{-}\gamma$ coincidence techniques: one using a proportional counter (PC) as beta detector, the other using an LS counter as beta detector. The results of both methods agree and can be considered to be model-independent in the sense, that they do not require any information about the beta spectrum shape. In addition, CNET and TDCR measurements were carried out using various counters.

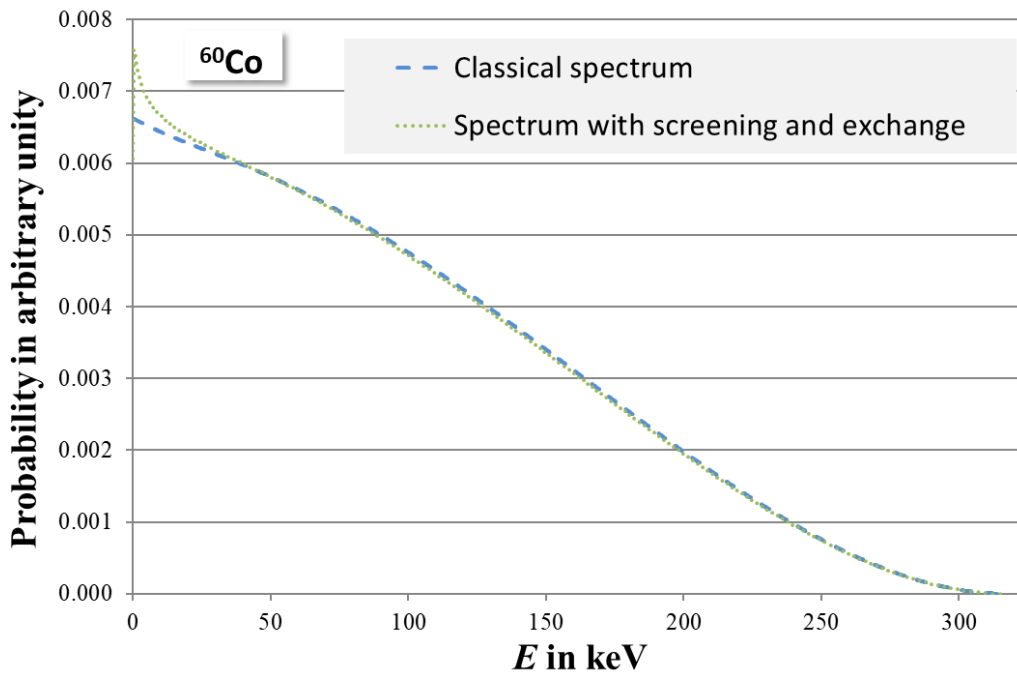


Figure 34: Computed beta spectra for ^{60}Co . The classical spectrum (dashed line) was calculated without any correction, whereas the second spectrum (dotted line) calculated with the BetaShape code takes the atomic exchange effect and screening correction into account.

When using the classical beta spectrum for the dominant allowed beta transition (blue dashed curve in Figure 34), one observes a significant trend when varying the counting efficiency and the LS-based result are not in agreement with the coincidence counting result, which is represented as the blue solid line in Figure 35. Again, the situation only improves, when using a beta spectrum which was calculated with the BetaShape code taking into account the screening correction and atomic exchange effect.

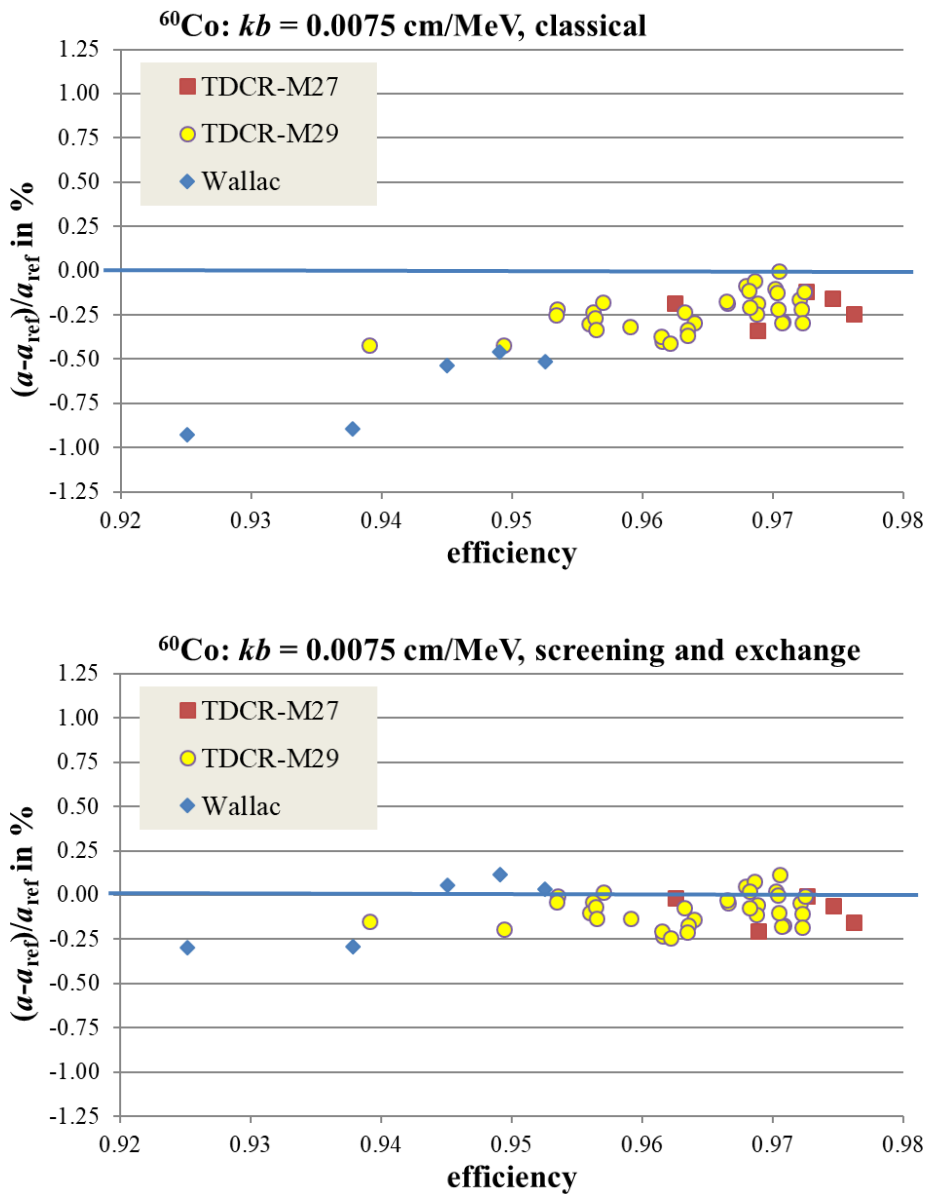


Figure 35: Relative deviation between the activity concentrations determined from individual ^{60}Co LS samples and a reference value (blue solid line at 0) obtained as the mean of two coincidence counting methods. The LS data were analysed with the classical beta spectrum (top) and a beta spectrum taking the atomic exchange effect and screening correction into account (bottom). In both cases, $kB = 0.0075 \text{ cm MeV}^{-1}$ was used.

When changing the parameter kB from 0.0075 cm/MeV to 0.0110 cm/MeV , the determined activity concentration increases for TDCR while it decreases for CNET. Hence, the mean value is rather robust which demonstrates the advantage when using both techniques rather than just one of them. In the case of ^{63}Ni

(Figure 33) one can also see that using just one method might not be sufficient. Assuming that a laboratory is just applied the TDCR method and used the classical beta spectrum, then in this case, the results would be in agreement (i.e. no trend when varying the efficiency), but the results would be wrong.

The preliminary results of the MMC measurements for ^{99}Tc are shown in Figure 36. The spectrum obtained at CEA (red) has an excellent energy resolution showing sharp peaks from the external ^{133}Ba reference source plus Pb fluorescence and Au escape peaks. The preliminary MMC result from PTB shown in Figure 36 (black) has a worse energy resolution which can be identified by the rather wide peak of the ^{241}Am reference source. The two spectra, however, agree in general. The preliminary data from the magnetic spectrometer at CHUV obtained in this project (blue) and a spectrum obtained using a shape-factor function from Reich and Schüpferling (1974) are also shown (magenta).

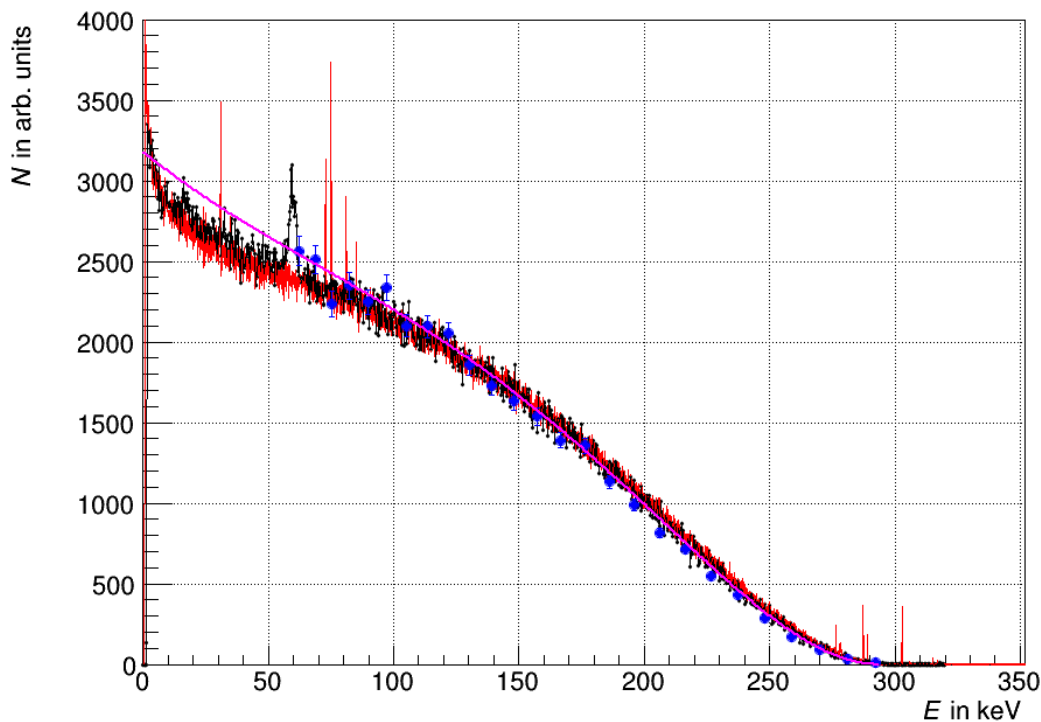


Figure 36: Experimentally determined beta spectra for ^{99}Tc , including preliminary data from this project.

In the following, the MMC spectrum from CEA will be used for an analysis of LSC data. To this end, the spectrum was first modified to remove the photon peaks. Then, a shape-factor function was determined. It was not possible to find an appropriate shape-factor function which describes the entire spectrum. Hence only the high energy part of the spectrum between 100 keV and 290 keV was used. The fit result is shown in Figure 37. When using the determined shape-factor function, it was possible to make a pseudo Kurie plot (Figure 38). This is required to determine a maximum energy which was found to be 295.1 keV. This result is slightly higher than the evaluated DDEP value of 293.8 keV and lower than the value 297.5 keV stated in the AME2016 atomic mass evaluation.

The resulting beta spectrum, i.e. the spectrum between ~ 0 keV and 295.1 keV measured by means of MMCs after removal of the photon peaks, was then used to analyse a set of experimental LS data. In addition, the shape-factor $q^2 + 0.54 \cdot p^2$ according to Reich and Schüpferling (1974) with a maximum beta energy of 293.8 keV was used (see Figure 39 and Table 1).

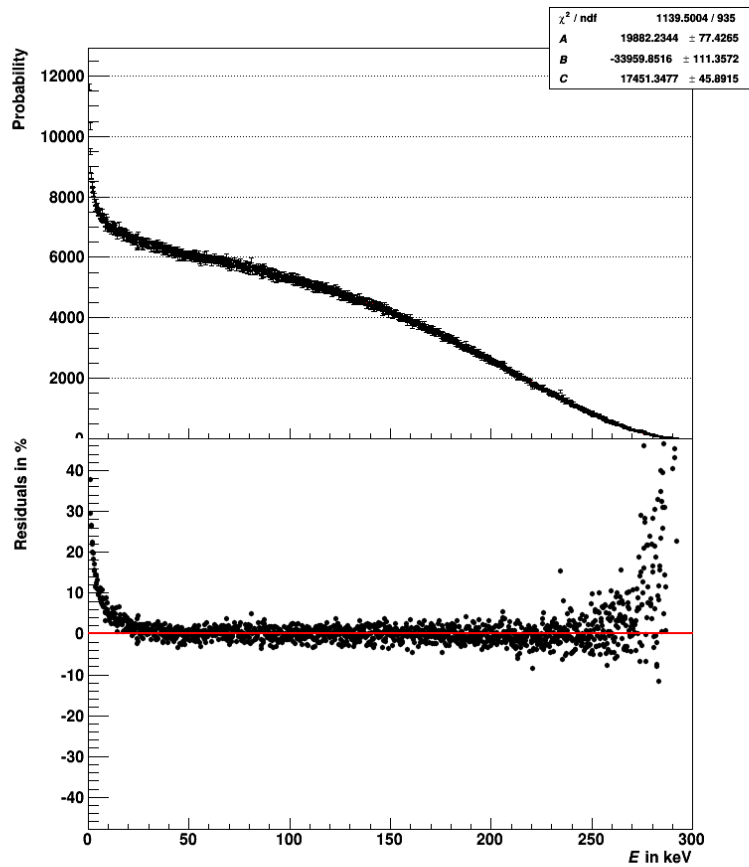


Figure 37: The MMC-based spectrum from CEA was used to determine a shape-factor function for the high-energy part. This function is needed to determine the maximum energy by means of a Kurie plot (see Figure 38).

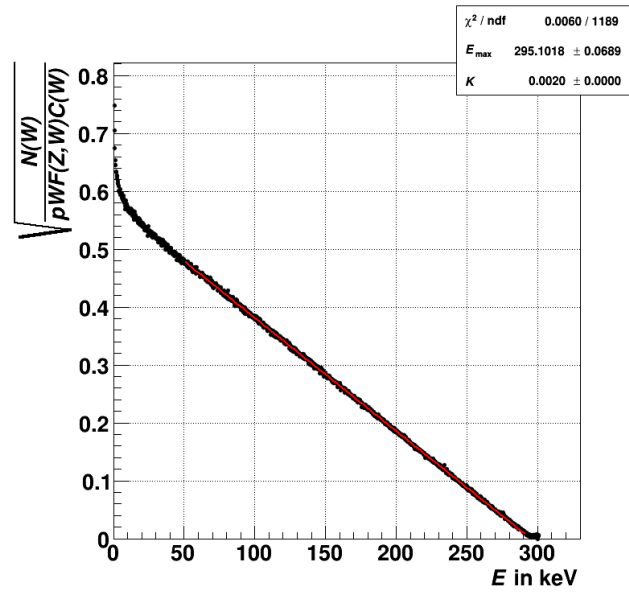


Figure 38: Pseudo-Kurie plot using the MMC-based spectrum from CEA and the shape-factor function from a fit (only the high-energy part of the spectrum in Figure 37).

When using the Reich and Schüpferling spectrum the activity concentration determined using the Wallac CNET counter is a bit higher than that obtained from TDCR-M27. The agreement between these two counters is much better when using the MMC based beta spectrum. It should, however, be noted that the situation looks slightly different when using a TriCarb 2800 TR for CNET. In this case, the agreement appears to be better when using the Reich and Schüpferling spectrum. It is difficult to judge which of the commercial counters gives the better answer (at PTB usually the Wallac counter is the preferred system). Hence, we can just calculate a mean activity concentration of all CNET results. The outcome (see Table 1) shows, that the relative deviation is slightly lower when using the MMC-based beta spectrum.

In general, the MMC-based spectrum yields slightly lower values for the activity concentration. For this study on ⁹⁹Tc, the effect is very low when applying the TDCR method.

Table 1: Activity concentration of a ⁹⁹Tc solution determined by CNET using a Wallac (W) and a TriCarb 2800 TR (T1) counter and by TDCR using M27 of PTB. Two beta spectra were used for the analysis.

Method/Counter	a in kBq/g when using MMC-based beta spectrum	rel. deviation between result and TDCR	a in kBq/g when using R+S-based beta spectrum	rel. deviation between result and TDCR
CNET/W	169.1	0.10 %	169.6	0.29 %
CNET/T1	168.7	-0.16 %	169.1	0.00 %
CNET/W+T1	168.9	-0.03 %	169.4	0.14 %
TDCR/M27	168.9		169.1	

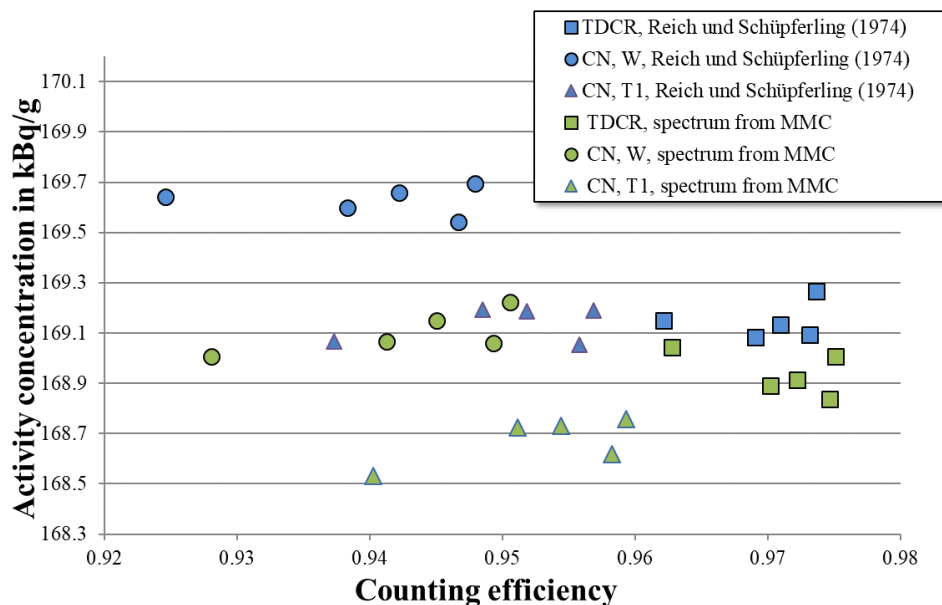


Figure 39: Activity concentration of a ⁹⁹Tc solution as a function of the counting efficiency when using a *kB* parameter of 0.0075 cm/MeV.

The above analysis shows the effect of improved beta spectra on absolute activity measurements. When using incorrect beta spectra, the determined activity can be significantly biased. For ⁶³Ni, this bias can be in the order of about 1 %, which is larger than the uncertainty estimated in some NMIs/DIs when standardising this radionuclide by means of LS counting. In the case of ⁹⁹Tc, the influence of the beta spectrum is lower, however, the effect is in the order of about 0.3 % for CNET and of about 0.12 % for TDCR. In a comparison exercise on the same set of TDCR data, three participants estimated overall relative standard uncertainties of 0.25 % or lower, with the lowest estimated uncertainty of 0.14 %. Hence, the effect of the beta spectrum must be

considered as being significant. The beta spectrum also matters when standardising ^{60}Co by means of LS counting where the effect can be in the order of 0.5 %.

An important conclusion is that this study underpins the need for extended research in the field of beta spectra to obtain better experimental data as well as better calculation tools for further radionuclides.

Bremsstrahlung cross-section measurements

Monte Carol simulations of the Bremsstrahlung cross-sections were performed using Geant4 and the measurement device was fully commissioned and calibrated in terms of energy and efficiency. Unfortunately, the radioactive source available for these measurements, a ^{90}Sr source with an activity of 37 MBq, produced a simulated Bremsstrahlung production rate of only 100 photons per day, meaning that no measurements were feasible. A new source of 10 GBq was ordered, but was not delivered before the end of the project. These studies have been reported in full detail.

5 Impact

Information on the project and various results has been presented at many national and international meetings. The following three ICRM Working Groups: Nuclear Decay Data, Beta Spectrometry and Life Sciences in 2017, 2018 and 2019; the JEFF Working Group of the OECD/NEA at a number of their biannual meetings; the Technical Committee for Ionising Radiation of the European Metrology Organisation, as well as at two meetings of the International Atomic Energy Agency's Nuclear Structure and Decay Data Network (2017 and 2019) and the German Physical Society Spring 2018 Meeting on Condensed Matter Physics.

Presentations were also given at several International Conferences: Advances in Liquid Scintillation Counting (LSC 2017), Denmark, May 2017; Radionuclide Metrology (ICRM 2017), Argentina, May 2017 and Radionuclide Metrology (ICRM 2019), Spain, May 2019; International Conference on Nuclear Data and Its Applications, China, May 2019; Low Temperature Detectors (LTD-17), Japan, July 2017 and Low Temperature Detectors (LTD-18), Italy, July 2019; Ultra Low Temperature Physics (ULT-2017), Germany, August 2017 and the 4th International Workshop on Superconducting Sensors and Detectors, Australia, July 2018.

A number of peer-reviewed conference proceeding articles have been published resulting from these presentations.

Impact on industrial and other user communities

Precisely determined mean beta energies, deduced from the spectral shape and with the end-point energies, are important to the nuclear power industry. The data made available from this project will help to reduce the uncertainties on the calculation of the residual decay heat in nuclear reactors that is in the large part due to beta emission after reactor shutdown. In this way, post-irradiation fuel management will be improved and made more cost-efficient. The Joint Evaluated Fission and Fusion (JEFF) project of the OECD Nuclear Energy Agency produces the reference nuclear data libraries used within Europe. The next release of the Radioactive Decay Data sub-library will contain evaluations, which have used the BetaShape code to calculate the beta spectra and associated mean energies.

The precise beta spectra from this project are also being used to reduce unnecessary doses being delivered when beta-emitting radiopharmaceuticals are used for diagnosis or treatment in nuclear medicine, particularly in the treatment of cancer.

The environmental measurement community are also benefitting from the better knowledge of beta spectra.

Impact on the metrology and scientific communities

Significant development work related to the metallic magnetic calorimeter (MMC) detection systems has been carried out and a completely new cryogenic system has been installed and commissioned. The lessons learnt have been documented and made available as a "Good Practice Guide", ensuring knowledge transfer to other laboratories wishing to establish an equivalent system. This Guide has already been supplied to Los Alamos National Laboratory and Lawrence Livermore National Laboratory upon their request. Specifically designed chips for this project were manufactured and subsequent design modelling work showed the expected energy resolution to be better than originally expected, i.e. 20 eV (instead of 60 eV) and 90 eV (instead of 200 eV), for the two types originally specified for measuring the different energies. In reality, five different chips, have been produced, meaning that a more refined choice for each radionuclide (and endpoint energy) could be

made. A number of these new chips were used for the measurements made during the project, for example, C-14, Tc-99 and Sm-151. An additional source preparation technique, not originally planned in the project, using gold nano-foams, was studied.

A new version of the BetaShape code, which can be used to calculate improved beta spectra, has been made available from the CEA website: <http://www.lnhb.fr/rd-activities/spectrum-processing-software/>. The code was used to calculate the Co-60 beta spectrum and these initial results from the project have already demonstrated the impact on the determination of the becquerel through activity measurements carried out using liquid scintillation counting for Co-60.

Measured spectra have been obtained for a number of radionuclides using a variety of different techniques, as already reported in this summary. These spectra will be useful in constraining further theoretical developments to be included in future versions of the BetaShape code, and also for ensuring accurate absolute activity measurements can be performed for the radionuclides in question, since these spectra are required for the liquid scintillation counting method – a robust method used regularly in many National Metrology Institutes (NMIs).

Impact on relevant standards

The project has had a direct and demonstrated impact on the primary activity standard measurements for pure beta emitters, carried out using the liquid scintillation counting technique, as has clearly been demonstrated for Co-60. This technique is the main method for activity measurements in most National Metrology Institutes (NMIs) and so adoption of the beta spectra calculated and/or measured in this project will be paramount. Their use has been promoted to the relevant bodies, e.g. CCRI(II) of the BIPM, EURAMET Technical Committee on Ionising Radiation, and working groups of the ICRM, etc.

Longer-term economic, social and environmental impacts

A number of “Good Practice Guides” have been produced describing the various developments to the experimental techniques used in this project. In addition, the precisely measured beta spectra, and their associated uncertainties, are now available, to allow their use in metrology laboratories and the relevant industries. A “Validation Report” on the effect of improved beta spectra on absolute activity measurements has been produced and will help improve the quantification of the associated uncertainty component in the measured activity standard. The project has provided stakeholders and end users in research establishments, the nuclear industry and the medical community with new nuclear data and methods for more precise activity measurements (the becquerel) of beta-emitting radionuclides using different measurement techniques, e.g. liquid scintillation counting and Si(Li) detectors. Targeted stakeholder groups have been preferentially addressed, including the broader scientific community, National Metrology Institutes, nuclear power plant operators, radioactive waste agencies, nuclear medicine clinics, environmental agencies and food and water measuring laboratories.

6 List of publications

1. I. Dedes, J. Dudek, *Narrowing the confidence intervals in nuclear structure predictions through elimination of parametric correlations*, Acta Physica Polonica B Proc. Supp. **10** (2017) 51
<http://dx.doi.org/10.5506/APhysPolBSupp.10.51>
2. K. Kossert, J. Marganec-Gałązka, X. Mougeot, O.J. Nähle, *Activity determination of ⁶⁰Co and the importance of its beta spectrum*, Applied Radiation and Isotopes **134** (2018) 212
<http://dx.doi.org/10.1016/j.apradiso.2017.06.015>
3. P. Novotny, P. Dryak, J. Solc, P. Kovar, Z. Vykydal, *Characterization of the Si(Li) detector for Monte Carlo calculations of beta spectra*, Journal of Instrumentation **13** (2018) P01021
<http://dx.doi.org/10.1088/1748-0221/13/01/P01021> also available at <https://arxiv.org/abs/1904.01294>
4. J. Dudek, I. Dedes, J. Yang, A. Baran, D. Curien, T. Dickel, A. Gózdź, D. Rouvel, H.L. Wang, *High-rank symmetries in nuclei: challenges for prediction capacities of the nuclear mean-field theories*, Acta Physica Polonica B **50** (2019) 685
<http://dx.doi.org/10.5506/APhysPolB.50.685>
5. R. Sandler, G. Bollen, J. Dissanayake, M. Eibach, K. Gulyuz, A. Hamaker, C. Izzo, X. Mougeot, D. Puentes, F. G. A. Quarati, M. Redshaw, R. Ringle, I. Yandow, *Direct determination of the ¹³⁸La β-decay Q value using Penning trap mass spectrometry*, Physical Review C **100** (2019) 014308
<http://dx.doi.org/10.1103/PhysRevC.100.014308> also available at <https://arxiv.org/abs/1904.12076v2>

6. F. Juget, G. Lorusso, G. Haefeli, Y. Nedjadi, F. Bochud, C. Bailat, *Development and validation of a double focalizing magnetic spectrometer for beta spectrum measurements*, Nuclear Instruments and Methods in Physics Research A **942** (2019) 162384
<https://doi.org/10.1016/j.nima.2019.162384>
7. M. Paulsen, J. Beyer, L. Bockhorn, C. Enss, S. Kempf, K. Kossert, M. Loidl, R. Mariam, O. Nähle, P. Ranitzsch and M. Rodrigues, *Development of a beta spectrometry setup using metallic magnetic calorimeters*, Journal of Instrumentation **14** (2019) P08012
<https://doi.org/10.1088/1748-0221/14/08/P08012>
8. I. Dedes, J. Dudek, *Propagation of the nuclear mean-field uncertainties with increasing distance from the parameter adjustment zone: Applications to superheavy nuclei*, Physical Review C **99** (2019) 054310
<https://doi.org/10.1103/PhysRevC.99.054310>
9. D. Rouvel, J. Dudek, *New approach to the adiabaticity concepts in the collective nuclear motion: Impact for the collective-inertia tensor and comparisons with experiment*, Physical Review C **99** (2019) 041303(R)
<https://doi.org/10.1103/PhysRevC.99.041303>
10. M. Loidl, J. Beyer, L. Bockhorn, C. Enss, S. Kempf, K. Kossert, R. Mariam, O. Nähle, M. Paulsen, P. Ranitzsch, M. Rodrigues, M. Schmidt, *Beta Spectrometry with Metallic Magnetic Calorimeters in the Framework of the European EMPIR project MetroBeta*, Applied Radiation and Isotopes **153** (2019) 108830
<https://doi.org/10.1016/j.apradiso.2019.108830>